Supplemental Materials and Methods

Supplemental abbreviations:

Δ12-PGJ2, Δ12-Prostaglandin J2; **5HETE**, 5-hydroxyeicosatetraenoic acid; **5oxoETE**, 5-oxoeicosatetraenoic acid; **6kPGF1α**, 6-keto-prostaglandin F1α; **6trans12epiLTB4**, 6-trans-12-epi leukotriene B4; **9HODE**, 9-hydroxyoctadecadienoic acid; **12HETE**, 12-hydroxyeicosatetraenoic acid; **13,14dihydro15ketoPGD2**, 13, 14-dihydro-15-keto prostaglandin D2; **13,14dihydro15ketoPGE2**, 13, 14-dihydro-15-keto prostaglandin E2; **13,14dihydro15ketoPGF2α**, 13, 14-dihydro-15-keto prostaglandin F2α; **13HODE**, 13-hydroxyoctadecadienoic acid; **14SHDHA**, 14S-hydroxydocosahexaenoic acid; **15HETE**, 15-hydroxyeicosatetraenoic acid; **15dPGJ2**, 15-deoxy-Δ12,14-Prostaglandin J2; **15ketoPGE2**, 15-keto-prostaglandin E2; **17SHDHA**, 17S-hydroxydocosahexaenoic acid; **LTB4**, leukotriene B4; **LTC4**, leukotriene C4; **LTE4**, leukotriene E4; **LXA4**, lipoxin A4; **LXB4**, lipoxin B4; **MaR1**, 7(S)-maresin; **MCSF**, macrophage colony stimulating factor; **PDx**, 17(S)-protectin; **PGD2**, prostaglandin D2; **PGE2**, prostaglandin E2; **PGE3**, prostaglandin E3; **PGF2α**, prostaglandin F2α; **PGJ2**, prostaglandin J2; PGPC, 1-palmitoyl, 2-glutaryl phosphatidylcholine; **rMCSF**, recombinant macrophage colony stimulating factor; **RvD1**, resolvin D1; **RvD2**, resolvin D2; **RvD3**, resolvin D3; **RvD4**, resolvin D4; **RvD5**, resolvin D5; **RvE1**, resolvin E1; **TXB2**, thromboxane B2; **TXB3**, thromboxane B3.

MRM LC-MS/MS Pro-Inflammatory and Inflammation Resolving Lipid Signaling Panel

Overview

Several groups have recently developed ESI LC-MS/MS methods for collectively analyzing various arachidonic acid (AA), DHA, and EPA-derived signaling lipids (AA and EPA-derived eicosanoids as well as DHA-derived docosanoids), which cover a range of pro-inflammatory, anti-inflammatory, and

inflammation resolving bioactive lipids.(1-6) Each of these groups uses multiple reaction monitoring (MRM) in negative ion mode coupled together with liquid chromatography as the basis for identification and quantification. Chromatography is performed on C18 column variants, with gradient elutions consisting of water and either methanol or acetonitrile, all together with formic or acetic acid. A certain number of deuterated internal standards are used to compensate for variability in sample preparation, injection volume, and ionization efficiency. Most all sample preparation methods involve some form of solid-phase extraction (SPE).

We settled upon the analytes of our lipid panel by cross-reference to the above cited methods, together with a more general search of the literature regarding eicosanoid, anti-inflammatory lipid, and specialized pro-resolving lipid mediator (SPM) biology.(7-10) We sought to analyze the bioactive lipids detailed in the body of this paper (see Table 1). However, several of these lipids are unstable or with short half-lives in either tissue or plasma. For example, PGI2 is bioactive but unstable and rapidly hydrolyzes to 6ketoPGF1α. Likewise, PGE2 is converted to both 15ketoPGE2 and 13,14-dihydro-15keto-PGE2 in plasma. In these cases, we substituted or supplemented our analysis of a particular bioactive lipid with analysis of its degradation products (see Supplemental Table 1 for a complete list). We also included various pathway markers in our analysis, for example: 14-HDHA and 17-HDHA as markers for the DHA → MaR1, and RvD-14 and PD1/PDx pathways, respectively(11); and 11 HETE as a monohydroxylated marker of COX activity.(12)

The method covers 39 distinct bioactive lipids, degradation products, and pathway markers. We divided the bioactive lipids into pro-inflammatory, anti-inflammatory, and pro-resolving functional categories by literature search (see Supplemental Table 1), while further indexing these as being COX or LOX products and as being derived from AA, DHA, or EPA (see Supplemental Table 1). We assigned each analyte to one of 19 distinct structurally identical or class-specific deuterated internal standards (see Supplemental Table 2). In the cases in which a particular analyte lacked a structurally identical internal

standard, we assigned an internal standard that both shared the same basic structure and co-eluted within 0.5 min of the analyte in question. For example, we assigned PGE2-d4 both to PGE2 and to PGF2α, which elutes within 0.3 min of PGE2-d4 and differs from PGE2 only by substitution of a ketone for a hydroxyl group within the cyclopentane ring (see Supplemental Table 2).

We built the method with two distinct MRM transitions for each analyte and internal standard, while MS/MS settings were optimized for declustering potential (DP), entrance potential (EP), collision energy (CE), and cell exit potential (CXP) by manual tuning (see below, and Supplemental Table 2). In the case of isobaric parent ions, distinct compounds were resolved by the use of either a unique MS2 fragment ion or by chromatographic separation. For example, the LOX products 15HETE and 12HETE both have a parent mass to charge (m/z) of 319.1, but these two species can be resolved through the use of the unique fragments of 219.1 for 15HETE and 184 for 12HETE. Chromatography on a Phenomenex Kinetex C18 column using a water and acetonitrile gradient gave sharp peak resolution (see Supplemental Figure 6). In order to ensure adequate dwell time for each MRM channel while also ensuring adequate data coverage of each chromatographic peak, we made use of scheduled MRM to activate only the requisite MRM channels within a 60 second window around each peak. For each analyte, we determined the LLOD, LLOQ, and ULOQ, while also determining the linearity of the associated standard curve (see Supplemental Table 3).

We prepared tissue, plasma, and lysate samples first by combination with methanol and the anti-oxidant butylated hydroxytoluene (BHT), and then by SPE using Oasis HLB cartridges. Post SPE, samples were reconstituted in methanol for LCMS analysis. We validated our sample preparation methods for each matrix by determining precision for each biologically available analyte across 5 identical extractions of a particular sample (see Supplemental Table 4), while also determining the precision and extraction efficiency of each internal standard within each matrix (see Supplemental Table

5). In accord with FDA guidelines, we set a CV of 15% as our cutoff for precision, while also ascertaining that recovery was consistent, precise, and reproducible.(13)

Chemicals

18-hydroxyeicosapentaenoic acid (18-HEPE); 6-keto-prostaglandin F1α (6kPGF1α); resolvin E1 (RvE1); resolvin E1 deuterated (RvE1-d4); thromboxane B3 (TXB3); thromboxane B2 (TXB2); thromboxane B2 deuterated (TXB2-d4); prostaglandin E3 (PGE3); 20-hydroxy-leukotriene B4 (LTB4); prostaglandin F2α (PGF2α); prostaglandin E2 (PGE2); prostaglandin E2 deuterated (PGE2-d4); resolvin D3 (RvD3); resolvin D3 deuterated (RvD3-d5); lipoxin B4 (LXB4), prostaglandin D2 (PGD2); prostaglandin D2 deuterated (PGD2-d4); resolvin D2 (RVD2); resolvin D2 deuterated (RvD2-d5); leukotriene C4 (LTC4); leukotriene C4 deuterated (LTC4-d5); 15-keto-prostaglandin E2 (15keto-PGE2); leukotriene E4 (LTE4); lipoxin A4 (LxA4); lipoxin A4 deuterated (LxA4-d5); 15-epi-lipoxin A4 (15epi-LXA4); resolvin D1 (RvD1); resolvin D1 deuterated (RvD1-d5); 13, 14-dihydro-15-keto prostaglandin F2α (13,14-dihydro-15keto-PGF2α); 13, 14-dihydro-15-keto prostaglandin F2α deuterated (13,14-dihydro-15-keto-PGF2α-d4); 13, 14-dihydro-15-keto prostaglandin E2 (13,14-dihydro-15keto-PGE2); 13, 14-dihydro-15-keto prostaglandin E2 deuterated (13,14-dihydro-15-keto-PGE2-d4); resolvin D4 (RvD4); 13, 14-dihydro-15-keto prostaglandin D2 (13,14-dihydro-15keto-PGD2); prostaglandin J2 (PGJ2); Δ12-Prostaglandin J2 (Δ12-PGJ2); 7(S)-maresin (MaR1); 7(S)-maresin deuterated (MaR1-d5); 10(S),17(S)-protectin (PDx); 6-trans-12-epi leukotriene B4 (6trans-12epi-LTB4); resolvin D5 (RvD5); leukotriene B4 (LTB4); leukotriene B4 deuterated (LTB4-d4); 15-deoxy-Δ12,14-Prostaglandin J2 (15d-PGJ2); 15-deoxy-Δ12,14-Prostaglandin J2 deuterated (15d-PGJ2-d4); 13-hydroxyoctadecadienoic acid (13-HODE), 9-HODE, 13-HODE-d4; 15-hydroxyeicosatetraenoic acid (15-HETE) and 12-HETE, 5-HETE, 15-HETE-d8, 12-HETE-d8, 5-HETE-d8, and 11-HETE; 17S-hydroxydocosahexaenoic acid (17S-HDHA) and 14S-HDHA; 5-oxoeicosatetraenoic acid (5-

oxoETE); and 5-oxoeicosatetraenoic acid deuterated (5-oxoETE-d7) were purchased from Cayman Chemicals (Ann Arbor, MI, USA).

Liquid Chromatography

Chromatography was performed on an Agilent 1290 UHPLC system using a Phenomenex Kinetex C18 column (2.6 uM particle size, 2.1 mm ID x 150 mm) and gradient elution. Solvent A was 75/25/0.1 (H2O/acetonitrile/formic acid) and Solvent B was 100/0.1 (acetonitrile/formic acid), and the gradient was as follows: 0-8.5 min, 0-85%B; 8.5-9.5 min, 85-100%B; 9.5-10.5 min, 100%B; 10.5-12 min, 100-0% B; 12-14 min, 0%B; with an additional 1 min equilibration at the starting conditions prior to each run. The column oven was set to 40 deg C, while the flow rate was 350 ul/min. 5 ul of sample was injected for each run.

MS/MS

Mass spectrographic analysis was performed on a SCIEX 5500 QTrap run in negative ion mode and controlled by Analyst 1.6.2 software. Two separate MRM transitions were determined for each compound, and DP, EP, CE, and CXP for each compound were all manually optimized by tuning on direct infusions of approximately 50 ng compound/ml 50%B (see Supplemental Table 2 for final settings). The source settings were optimized by tuning on a mix of analytes while also flowing in 50%B at 350 ul/min, with temperature set at x, GS1 at x, GS2 at x, CAD gas a medium and CUR gas at 25. Scheduled MRM was employed, with the window for each MRM channel set at 60 seconds around the retention times (RT) of each compound (see Supplemental Table 2 for RT). LLOD, LLOQ, ULOQ, and linearity of response for each analyte were determined (see Supplemental Table 3).

Sample preparation

Lipids were extracted from 50 mg of intestinal tissue by first adding 500 μl MS-grade H_20 together with 50 μl of 20 ng/ml internal standard mix as well as a final concentration of 20 uM BHT. The tissue was homogenized, 1 ml of methanol was added, the tissue was vortexed, and the sample was spun down at 15000 RPM for 10 min at 4^0C. The supernatant was removed and brought up to 10 ml with pH 3-4 HCl-acidified H_2O. SPE was performed on an Oasis HLB 3 cc column in accord with the manufacturer's protocol. The sample was eluted with 2 ml methanol, dried down under argon, and brought up again in 100 μl methanol for LCMS analysis. The final concentrations of internal standards in the samples were 10 ng/ml.

Lipids were extracted from 100 ul of plasma by first adding 50 ul of 20 ng/ml internal standard mix together with 150 μl of methanol. BHT was added to a final concentration of 20 μM. The sample was vortexed and spun down at 15000 RPM for 10 min at 4^0C. The supernatant was combined with 1.8 ml of HCl-acidified H_2O (pH = 3-4); SPE was performed on 3 cc Oasis HLB cartridges; and samples were eluted with methanol, dried down under argon, and brought up in 100 μl of methanol for LCMS analysis.

Cells grown in culture were first washed of media 2x with cold PBS. The cells were then scraped and collected in 50 mM phosphate buffer (pH 7.4) and kept at -80^0C for subsequent lipid analysis. For 300 μl of lysate, sufficient for macrophages grown in a well of a 6 well plate, 50 μl of 20 ng/ml internal standard together with 150 μl of methanol was added as well as 20 μM BHT (final concentration). The samples were otherwise extracted as plasma.

1 ml of cell culture media was combined with 50 μl of internal standard mix together with 450 ul of methanol and 20 μM BHT (final concentration). The samples were vortexed, spun down, and supernatant was brought up to 5 ml with H2O. The samples were acidified to pH 3-4 using formic acid and otherwise extracted as above.

Each sample preparation method was independently validated by determining precision and recovery, as described above (see Supplemental Tables 4 and 5 for partial data).

Data analysis

Data analysis was performed using MultiQuant software, with the concentration of each analyte being determined relative to its internal standard and against standard curves. Final data was normalized to tissue weight, plasma volume, media volume, or for lysate protein concentration as determined by Bradford from a small aliquot of each lysate. For comparison between groups (see Figures 2, 4, and 9), statistical analysis was performed as described in the Methods of the main text.

MRM LC-MS/MS method for determination of oxPAPC species

Sample preparation

A biphasic liquid/liquid extraction method employing butanol was used to isolate oxPAPC species from both intestinal tissue and plasma (14). For intestine, 100 mg of tissue was combined with 100 μl of HPLC grade water and 300 μl of HPLC grade 1-butanol together with 30 μl of internal standard mix (500 ng/ml). Tissue was homogenized. 400 μl of brine (10% NaCl) and 300 μl of 1-butanol were added, and the sample was vortexed for 1 minute. Following centrifugation in glass tubes at 2000 rpm for 10 min, the upper organic phases were transferred to new glass tubes. The butanol was evaporated under argon, and the samples resolubilized in 150 μl methanol. The methanol was transferred to a new Eppendorf tube and centrifuged at 14000 rpm for 10 min to pellet debris. Samples were then transferred to MS vials for analysis. For plasma, 100 μl of plasma was combined in a glass tube with 500 μl brine and 600 ul 1-butanol. Internal standard was added and the sample handled otherwise as for intestinal tissue.

LC-MS/MS

A method to quantify the oxidized products of 1-palmitoyl-2-arachidonoyl-sn-glycero-3-phosphocholine (PAPC) was developed using LC-MS/MS. Analysis was performed as before on an AB Sciex 5500 QTRAP mass spectrometer in tandem with an Agilent 1290 Infinity liquid chromatographer. MS analysis was performed in positive mode utilizing an unscheduled MRM scan. Chromatography was performed using a Kinetex C8 2.6um 100Å 150x3mm RP column over a 15 minute run. The method employs two solvents: Solvent A being 90%/5%/5% water/acetonitrile/2-propanol, and solvent B being 75%/25% 2-propanol/acetonitrile. The solvents were run at 300ul/min with the following gradient: initial conditions 40% A, followed by a 30 second loading hold before an 11 minute linear gradient to 0% A, before a 2-minute flush at 0%A, then a return to initial conditions. The injection volume was 10ul and the autosampler was maintained at 4C while the solvent temperature was set to 25^0C. Samples were combined as above with two internal standards that bracketed the elution range of the oxPAPC species under analysis: 06:0 PC-d22 (1,2-dihexanoyl-d22-sn-glycero-3-phosphocholine) and 17:0-20:4 PC (1-heptadecanoyl-2-(5Z,8Z,11Z,14Z-eicosatetraenoyl)-sn-glycero-3-phosphocholine) (Avanti 790427 and LM1002). The MS method was built from standards for three 3 known oxidation products of PAPC: 1-palmitoyl-2-(5'-oxo-valeroyl)-sn-glycero-3-phosphocholine (POVPC), 1-palmitoyl-2-glutaryl-sn-glycero-3-phosphocholine (PGPC), and 1-(Palmitoyl)-2-(5-keto-6-octene-dioyl) phosphatidylcholine (KOdiAPC) (Avanti 870606, 870602; Cayman 62945). The transitions monitored were 474.7/184.1 and 474.7/125.1 (6:0 D22 PC); 594.0/184.1 and 594.4/125.1 (POVPC); 610.4/184.1 and 610.4/125.1 (PGPC); 664.4/184.1 and 664.4/125.1 (KOdiAPC); and 796.8/184.1 and 796.8/125.1 (17:0/20:4 PC). Curtain gas was 20 psi, CAD gas was medium, GS1 was 50 psi, GS2 was 30 psi, IS voltage was 5500V, temperature was 450 degrees C, DP was 140 v, EP was 10 v, CXP was 15 volts. CE was 35 and 60 for the transitions of POVPC, PGPC, and KOdiAPC; and 35 and 35 for 6:0 D22 PC and 17:0/20:4 PC. Quantification was performed using Analyst and MultiQuant software.

Human intestinal crypt isolation and enteroid cultures.

Intestinal crypt isolation. Small intestinal crypts were isolated as previously described (15, 16). Briefly, crypts were resuspended in basic medium (Advanced Dulbecco's Modified Eagle Medium (ADMEM)/Ham's F12 (Invitrogen) with 2 mM GlutaMAX (Invitrogen), 10 mM HEPES (Invitrogen). Crypt yield was determined by microscopic counting.

Cell culture. A thin film of liquid type I collagen (Advanced BioMatrix, San Diego, CA) was plated onto the bottom surface of 48-well Nucleon Delta-treated cell culture plate (Thermo Scientific, Waltham, MA) at a concentration of 100 ng/mL, incubated for 30 minutes, and then removed by aspiration. Human crypts were suspended within Matrigel at a concentration of 100 crypts per 25 µl of Matrigel and plated in 3D on the 48-well Nucleon Delta-treated cell culture plate. The crypts were grown with Human IntestiCult media from STEMCELL Technologies following manufacturers recommendations, and passaged every 7-9 days. These were grown as in Basic Medium with antibiotic-antimycotic (Invitrogen), 1 mM N-Acetylcysteine (Sigma), 100 ng/ml recombinant murine Noggin (PeproTech), 50 ng/ml recombinant murine EGF (PeproTech), 1xN2 supplement (Invitrogen), 1xB27 supplement (Invitrogen), 1 µg/ml recombinant human R-spondin 1 (R&D Systems, Minneapolis, MN), 10 µM Y-27632 inhibitor (Stemgent), 1 mM recombinant human Jagged-1 (R&D Systems), 5 µM CHIR99021 (GSK-3β inhibitor) (Stemolecule).

Additional Material and Methods

Basic IBD studies involving the *Cox2* CCHF and PAC *Il10*$^{-/-}$ mouse models. *Cox2* TKO or MKO mice were challenged with CCHF diet (Envigo TD.90221) for 2 or 7-10 weeks, respectively. Inflammation in the ileo-ceco-colic junctions was assessed by gross pathology, histological scoring of inflammation and epithelial damage (see below), as well as by immunohistochemistry for Ly6G and F4/80, and qPCR for TNFα and IL1β. Both immunohistochemistry and qPCR were performed in accord with standard protocols. C57BL/6J mice were fed the selective COX2 inhibitor celecoxib as described (17), and inflammation was

evaluated as below. Piroxicam was mixed into chow and fed to *Il10*$^{-/-}$ mice as described (18). On day 14, inclusive of an initial 9 day induction with piroxicam, colitis was evaluated in these mice as described in the Results section.

Barrier permeability, endotoxin, inflammation, and epithelial damage. For Figure 1B, ***Barrier permeability*** was measured by determining urinary excretion of sucralose, mannitol, and lactulose over 24 hours in metabolic cages following oral gavage. LC-MS/MS was used to determine the levels of these carbohydrates relative to raffinose, which was used as an internal standard. LC-MS/MS methods and dosing are as described (19), with modification involving the addition of sucralose (20). In a follow up study, we assessed barrier permeability by oral gavage of FITC-dextran 4 kD followed by fluorometric determination of this signal in serum (21). ***Endotoxin*** levels in portal vein serum were determined following collection of portal vein blood from anesthetized mice (22). Serum was allowed to form over 1 hour at RT. Serum samples were heated to 50°C for 10 min, and endotoxin levels were determined via limulus amebocyte lysate (LAL) assay in accord with the manufacturer's protocol (Kinetic Turbidimetric LAL Assay, Lonza). ***Inflammation*** and ***epithelial damage*** were determined by histological score of HE stained sections of ileo-ceco-colic junction. Inflammation was scored 0-4, taking into account severity, extent, and % area involved. Epithelial damage was also assessed separately on the basis of a score of 0-4 in three separate fields per sample (23). For this study alone, we necessarily scored inflammation and epithelial damage separately, as we were asking the question whether epithelial damage preceded intestinal inflammation.

H&E Disease Score. For all other histological analyses except for Figure 1B, inflammatory disease in the ileo-ceco-colic junctions was scored on a 0-12 scale on three separate fields per sample, involving the following criteria (24, 25): severity of inflammatory cell infiltrate into the lamina propria (0 = none; 1 =

mild; 2 = moderate; 3 = severe); extent of the inflammation: (0 = none; 1 = mucosal; 2 = mucosal and submucosal; 3 = transmural); % area involved (0 = none; 1 = up to 10%; 2 = up to 25%; 3 = above 25%); epithelial damage and altered mucosal architecture (0 = none; 1 = mild erosion of epithelium, minimal hyperplasia; 2 = moderate erosion of epithelium, mild to moderate loss of goblet cells, some crypt accesses; some villous blunting; 3 = crypt loss, moderate to severe ulceration, villous atrophy). Fractional sub-scores were permitted. Unlike the 0-4 point inflammatory score of Figure 1B, the 0-12 point H&E disease score takes into account damage or alterations to the epithelium and mucosa.

Antibiotic treatment. Vancomycin, ampicillin, neomycin, and metroniadazole were supplied in drinking water as described (26).

MyD88 inhibition. The MyD88 inhibitor T6167923 was supplied 3x/week at 250 μg/injection (27).

BML111 (LXA4 analog) rescue. The LXA4 analog BML111 (Tocris, 5488) was administered i.p. twice weekly to *Cox2* MKO mice across the course of 8.5 week CCHF challenge (n = 9) (28, 29). Inflammation in ileo-ceco-colic junctions of these mice was compared to that in FLOX and MKO mice on CCHF and chow (n=10/group). Ceca were evaluated histologically and also with respect to oxPAPC.

Macrophage studies. Mouse bone marrow derived macrophages (BMDM) (30) and peritoneal macrophages (PM) (31) were generated as previously described. Human THP-1 cells are a monocyte cell line that is commonly used to investigate mechanisms of the human innate immune response (32). Upon activation with phorbol 12-myristate 13-acetate (PMA), THP-1 cells differentiate into macrophage-like cells that respond similarly to primary macrophages upon exposure to pro-inflammatory stimuli like LPS or amyloid beta (33). (**Cell line**) Human THP-1 monocytes (ATCC, TIB-202) were grown in suspension

in accord with ATCC's protocol and differentiated to macrophages using 100 nM PMA. Both mouse and human macrophages were activated with 25 ng/ml LPS and co-treated with 15 μg/ml D-4F. For analysis of lipids, lysates and media were collected and assessed as described above. RNA was collected in Trizol, while protein lysate was in standard protein lysis buffer. Pro-inflammatory gene expression was determined using species-specific primers and BIoRad's SYBR green kit in accord with standard protocols. For both mouse and human macrophages, target gene expression was normalized to GAPDH, and results were expressed as fold-change compared to the relevant control. (**Antibodies**) Western blots were performed in accord with standard protocols using Cell Signaling mAb's against human-specific IκBα (#4814S, lot 17; mouse) with anti-mouse IgG HRP linked secondary antibody (#7076S, lot 34); and human GAPDH (#5174, lot 7; rabbit) with anti-rabbit IgG HRP linked secondary antibody (#7074, lot 28). THP-1 macrophages were also treated with 1 uM POVPC for 3 hours (34) with and without either D-4F or 3F(14) at 30 ug/ml, and IL1β and GAPDH expression were determined by qPCR.

Lipid inflammatory mediators in tissue and plasma of *Cox2* MKO and FLOX mice. Lipid inflammatory mediators were determined in both tissue and plasma of *Cox2* MKO and FLOX mice that had been fed a CCHF diet for 8.5 weeks (see above).

APOA1 mimetics and *Cox*2 MKO/CCHF. *Cox2* MKO mice were challenged with CCHF for 7, 8.5, and 10 weeks, and the effect of D-4F (500 μg/ml) on intestinal inflammation was determined as above. In brief, gross pathology; histopathology (HE inflammatory score and muscle thickness); IHC for Ly6G+, F4/80+, CD4+, and CD8+ leukocytes; and qPCR for expression of *Tnf* and *Il10* were determined. Lipid inflammatory mediators in both plasma and intestinal tissue were determined, as described. In a 3 week study, the effects of 4F on barrier permeability across each week (FITC-dextran method) as well as intestinal and plasma oxPAPC at 3 weeks were determined. Tg6F (0.06% w/w) in combination with

CCHF diet was fed to both *Cox2* MKO for 10 weeks or only during the final 5 weeks of the 10-week CCHF diet, and drug efficacy was assessed by gross pathology and histopathology.

***Apoa1* and *Duox2* and oxPAPC.** We performed an 8.5 week experiment to determine the levels of APOA1 protein and *Apoa1* gene expression, *Duox2* gene expression, and oxPAPC levels in MKO and FLOX mice on CCHF and chow. ApoA1 protein levels were determined for proximal colon, terminal ileum, and plasma by ELISA in accord with the manufacturer's protocol (Life Span Biosciences, LS-F5982). *Apoa1* and *Duox2* gene expression were determined by qPCR using previously published primer sequences. (*Duox2*: F = 5'-ACGCAGCTCTGTGTCAAAGGT-3', R = 5'-TGATGAACGAGACTCGACAGC-3' (35); *Apoa1*: F = 5'-GTGGCTCTGGTCTTCCTGAC-3', R = 5'-ACGGTTGAACCCAGAGTGTC-3' (36)). Levels of oxPAPC were determined as above.

THP-1 and human enteroid qPCR. For qPCR of human genes in the THP-1 and human enteroid experiments, we used the following primers: PTGS2-Fwd ATGCTGACTATGGCTACAAAAGC; PTGS2-Rev TCGGGCAATCATCAGGCAC; GAPDH-Fwd GGAGCGAGATCCCTCCAAAAT; GAPDH-Rev GGCTGTTGTCATACTTCTCATGG; TNFα-Fwd CAGAGGGCCTGTACCTCATC; TNFα-Rev GGAAGACCCCTCCCAGATAG; IL1β-Fwd GGGCCTCAAGGAAAAGAATC; IL1β-Rev TTCTGCTTGAGAGGTGCTGA; IL6-Fwd TACCCCAGGAGAAGATTCC; IL6-Rev TTTTCTGCCAGTGCCTCTTT; TLR4-Fwd TGAGCAGTCGTGCTGGTATC; TLR4-Rev CAGGGCTTTTCTGAGTCGTC.

Total cholesterol and PON1 activity. Both plasma TC and PON1 activity were determined as previously reported (37).

Ussing chamber experiments. These experiments were performed as previously published (18), except for the minor modifications detailed herein.

Binding affinity studies. Binding affinities between 4F and both cholate and 15HETE were determined by surface plasmon resonance in accord with methods previously detailed (38). Binding affinities between 4F and both LPS and lipid A were determined comparably, except that we calculated the equilibrium disassociation constants (K_D) by Biacore's affinity analysis—through determination of the half-maximum values of the plots of steady state levels versus analyte concentrations.

Assessment of colitis in PAC *Il10*$^{-/-}$ model. For the evaluation of the severity of colitis in the PAC *Il10*$^{-/-}$ model, we employed previously published procedures and criteria (18); see also Results in main text.

APOA1 mimetic 4F and PAC *Il10*$^{-/-}$. *Il10*$^{-/-}$ mice were pre-treated with D-4F (500 µg/ml drinking water) for 7 days. While continuing D-4F: colitis was induced for 9 days with piroxicam, and colitis and drug efficacy were assessed on day 14. For characterization of criteria for disease score, see Results in main text.

Heatmaps. Heatmaps of lipidomic data were generated using Clustvis (39).

Supplemental Figures

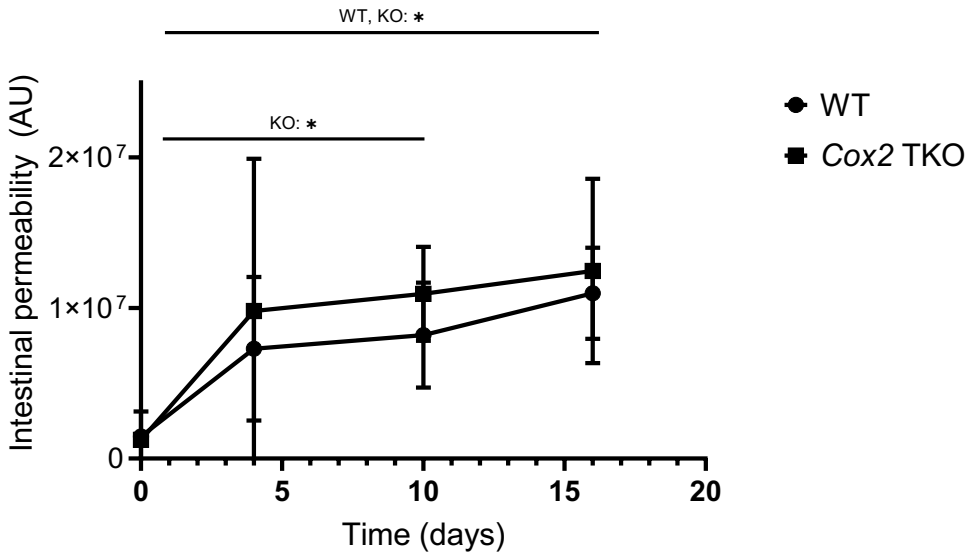

<u>Supplemental Figure 1.</u> CCHF increases barrier permeability in both *Cox2* TKO and WT mice. (*, $p < 0.05$) Both *Cox2* TKO and littermate control mice (WT) were challenged with CCHF diet over 16 days. Barrier permeability was determined over time by measuring via LC-MS/MS the level of sucralose excreted in urine over 24 hrs following oral gavage. Permeability significantly increased in both groups by day 16. (*Statistics*. Two-way ANOVA with Tukey's multiple comparisons test and adjusted p-values.)

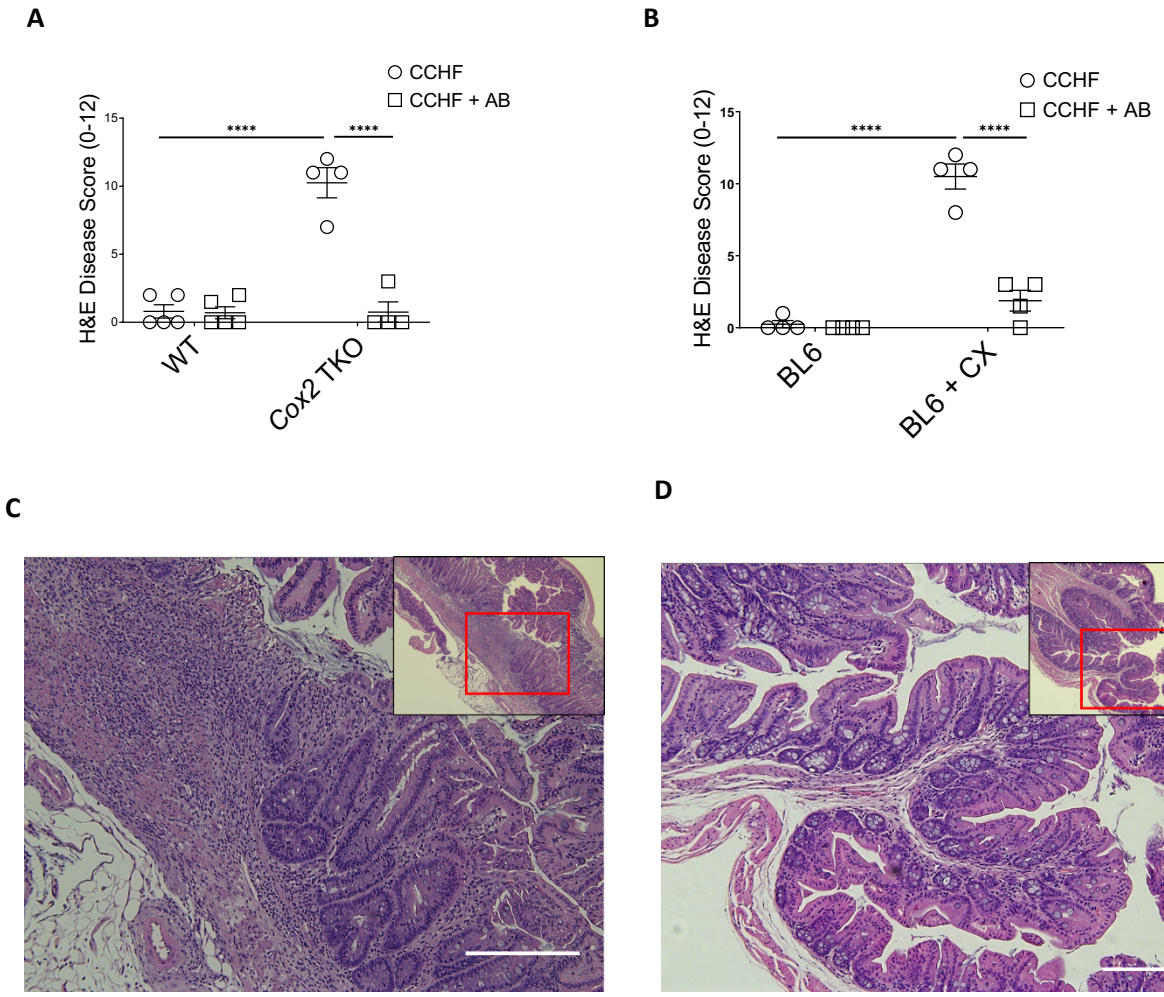

<u>Supplemental Figure 2</u>. Antibiotics abrogate intestinal inflammation in both *Cox2* TKO and CX-treated BL6 mice challenged with CCHF. (****, $p < 0.0001$) *Cox2* TKO or BL6+CX mice were pre-treated with vancomycin, ampicillin, neomycin, and metroniadazole for 7 days and continued on antibiotics (AB) for 14 days of CCHF (n = 4/group). AB abrogated intestinal inflammation in both *Cox2* TKO (**A**) and C57BL6 + CX (BL6 + CX) treated mice (**B**) as determined by H&E disease score**.** Representative images, BL6 + CX + CCHF (**C**) and BL6 + CX + CCHF + AB (**D**) (scale bar = 250 um). (*Statistics*. Two-way ANOVA with Tukey's multiple comparisons test and adjusted p-values.) (<u>Note</u>: (C) reproduces the image of Figure 1A *bottom panel*, whose representative image of the general effect of CCHF + CX in BL6 mice is taken from the above experiment.).

A

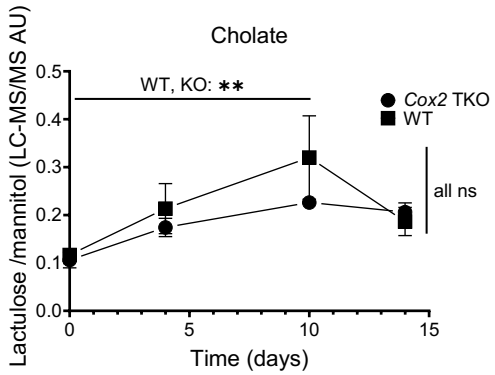

B

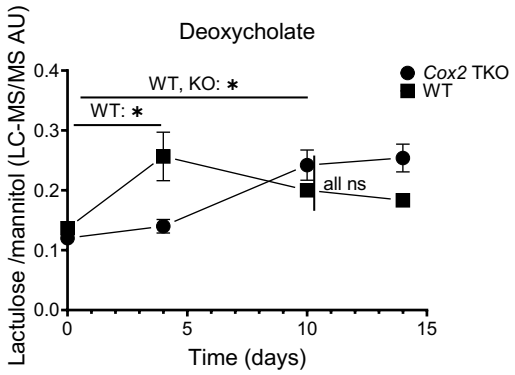

<u>Supplemental Figure 3</u>. Cholate and deoxycholate affect barrier permeability equally in both *Cox2* TKO and WT mice. (*, $p < 0.05$; **, $p < 0.01$) *Cox2* TKO and WT were pre-treated with antibiotics and then fed a chow diet containing either cholate (**A**) or deoxycholate (0.5% w/w) (**B**) while antibiotics were continued. Barrier permeability was determined at multiple time points by measuring the 24 hr urinary excretion of lactulose and mannitol by LC-MS/MS. Both diets significantly increased barrier permeability in both WT and KO mice by 10 days. There were no significant differences between any group at any time point (e.g., between cholate and deoxycholate *Cox2* TKO mice at 10 hrs). (*Statistics*. For comparison of either cholate or deoxycholate (KO v WT) across time, two-way ANOVA and Tukey's multiple comparisons test with adjusted p-values. For comparison of cholate and deoxycholate (KO v WT) at a time, one-way ANOVA and Tukey's multiple comparisons test.)

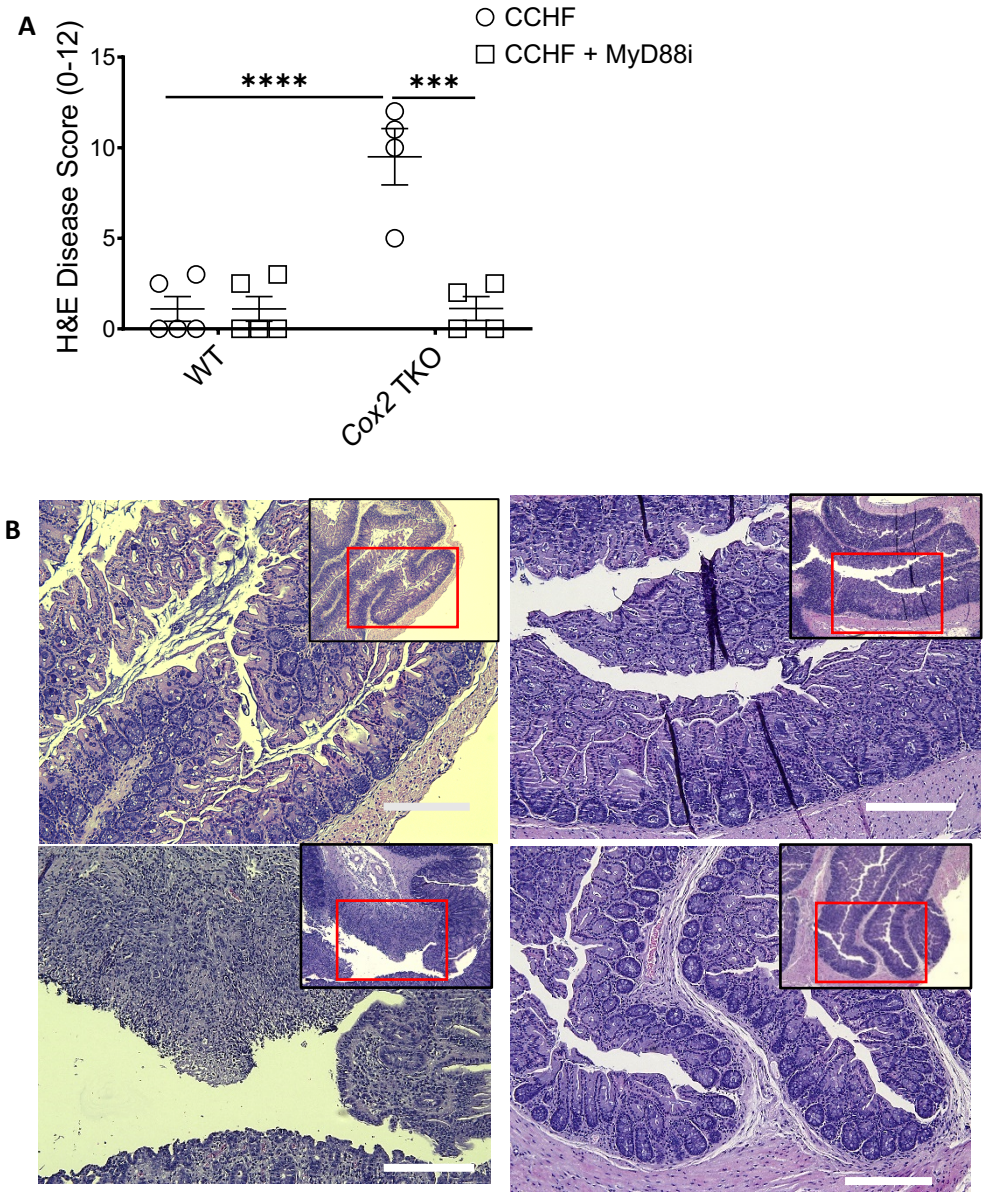

Supplemental Figure 4. MyD88 inhibition rescued intestinal inflammation in *Cox2* TKO + CCHF mice. (***, $p < 0.001$; ****, $p < 0.0001$) *Cox2* TKO and WT mice were fed CCHF diet for 14 days and treated with either vehicle or the MyD88 inhibitor T6167923 3x/wk i.p. (250 ug/injection). MyD88 inhibition significantly suppressed the development of inflammation in the ileo-ceco-colic junctions of *Cox2* TKO mice, as indicated by H&E disease score (**A**). Representative images: WT + CCHF (*upper left*); WT + CCHF + MyD88i (*upper right*); *Cox2* TKO + CCHF (*lower left*); *Cox2* TKO + CCHF + MyD88i (*lower right*) (scale bar = 250 um) (**B**) (*Statistics.* Two-way ANOVA with Tukey's multiple comparisons test and adjusted p-values). (Note: (B, *bottom left*) reproduces the image of Figure 1A *top panel*, whose representative image of the general effect of CCHF on *Cox2* TKO mice is taken from the above experiment.).

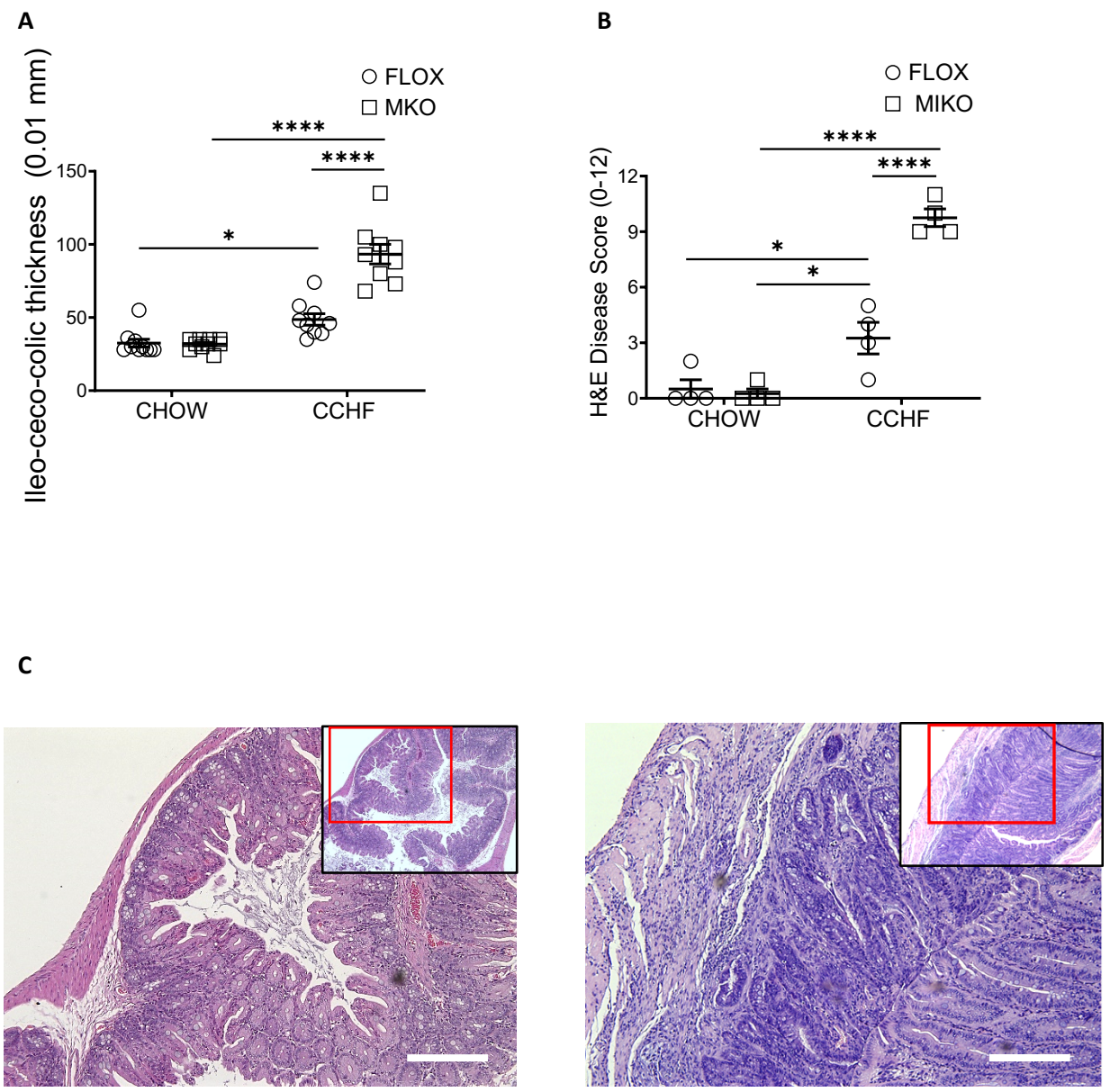

<u>Supplemental Figure 5.</u> ***Cox2*** **MKO mice develop severe inflammation in their ileo-ceco-colic junctions when challenged with CCHF diet for 7-10 weeks.** (*, $p < 0.05$; ****, $p < 0.0001$) Both *Cox2* MKO and FLOX mice were fed CCHF or chow for 8.5 weeks. *Cox2* MKO mice developed severe inflammation in their ileo-ceco-colic junctions as determined by gross pathology (**A**) and H&E disease score (**B**). The transmural disease was similar to that in *Cox2* TKO or CX + CCHF mice (**C**; representative images. *Left*, FLOX + CCHF; *right*, MKO + CCHF.) (Scale bar = 250 um) (*Statistics*. Two-way ANOVA with Tukey's multiple comparisons test and adjusted p-values).

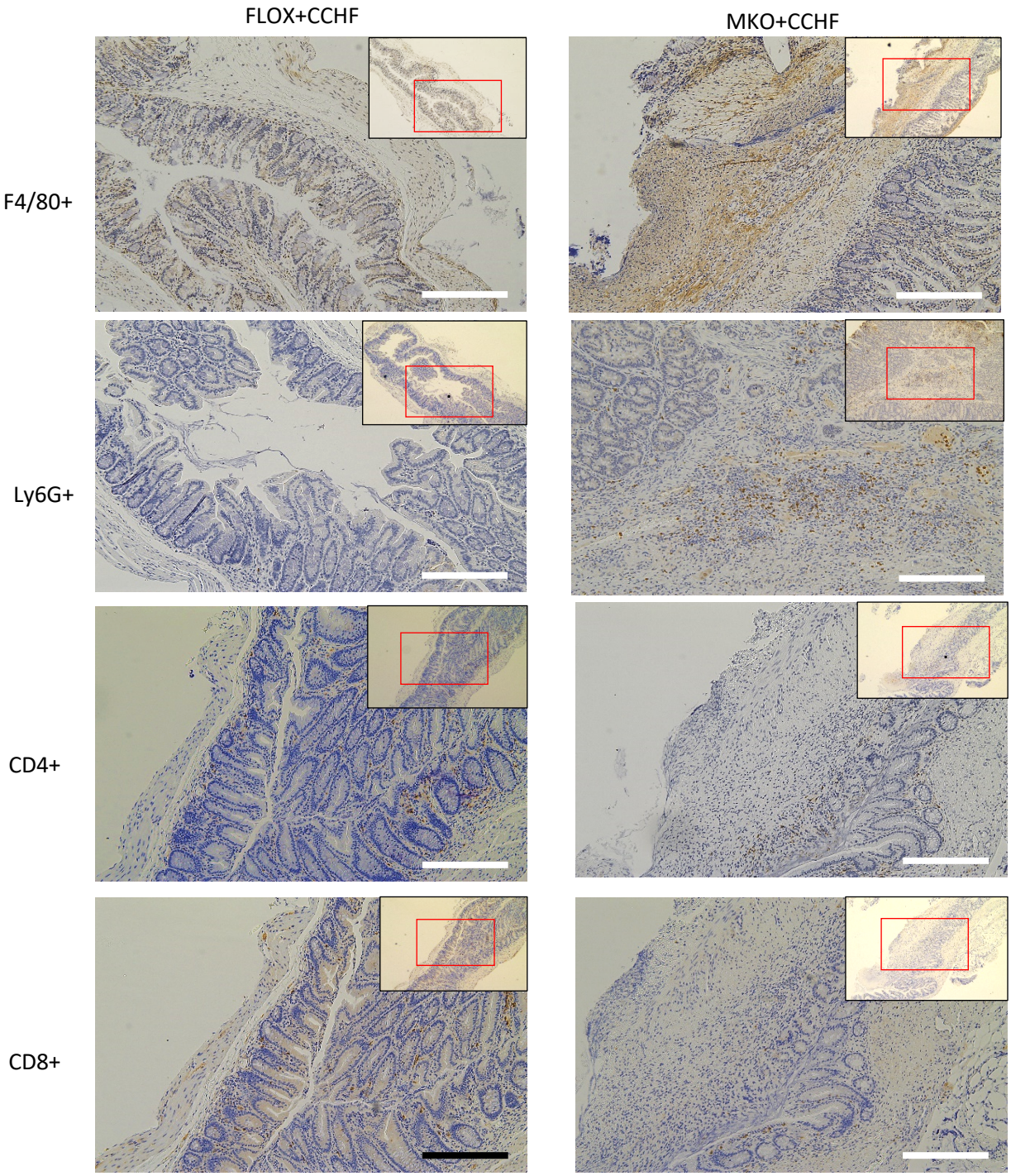

<u>Supplemental Figure 6.</u> Inflammatory lesions in the ileo-ceco-colic junctions of *Cox2* MKO + CCHF mice are characterized by expansion of macrophages and neutrophils but not CD4+ and CD8+ T cells. Ileo-ceco-colic junctions of MKO mice fed CCHF and CHOW were stained for macrophages (F4/80+), neutrophils (Ly6G+), and T lymphocytes (CD4+ and CD8+). Inflammatory lesions showed expansion of the macrophage and neutrophil but not T lymphocyte populations compared to FLOX + CCHF controls (representative images) (scale bars = 250 um). (<u>Note</u>: The panels above for F4/80+ and Ly6G+ in MKO + CCHF reproduce the panels of Figures 3D *left* and 3E *left*. For both this figure and Figure 3, these panels are equally representative of F4/80+ and Ly6G+ stain in MKO + CCHF mice.)

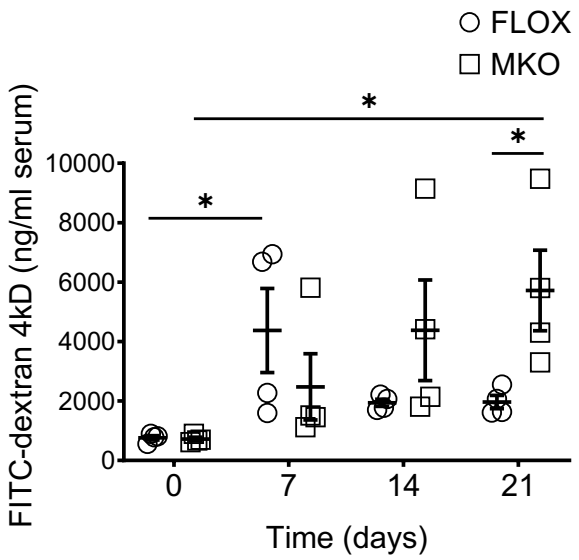

<u>Supplemental Figure 7.</u> CCHF impairs barrier function in both *Cox2* MKO and FLOX mice across 7 days, with permeability increasing in MKO vs FLOX mice by 21 days. (*, $p < 0.05$) Both MKO and FLOX mice were fed CCHF diet for 21 days. Both at baseline and again after 7, 14, and 21 days, mice were water fasted for 4 hours; gavaged with FITC-dextran 4 kD (440 mg/kg); and bled retro-orbitally after 4 hours. The amount of FITC present in serum was determined. CCHF significantly increased barrier permeability in both MKO and FLOX mice. By 21 days, permeability had significantly increased more in MKO compared to FLOX mice. (*Statistics*. For each of MKO and FLOX versus time, comparison of groups 7-21 days to 0 week baseline via one-way ANOVA with Dunnett's multiple comparisons test and adjusted p-values. For comparison of MKO versus FLOX at each time point, multiple t-tests with Holm-Sidak correction for multiple tests and adjusted p-values.)

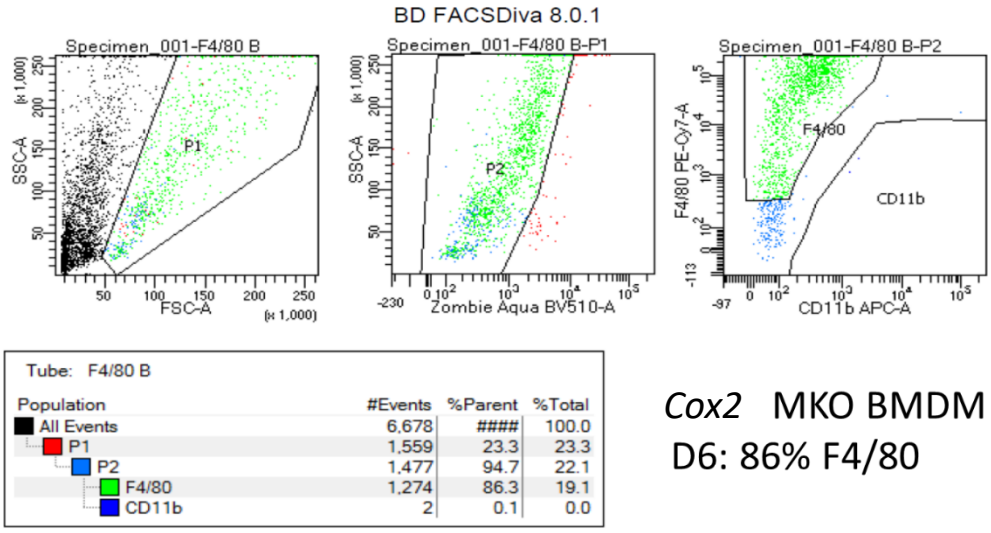

Tube: F4/80 B

Population	#Events	%Parent	%Total
All Events	6,678	####	100.0
P1	1,559	23.3	23.3
P2	1,477	94.7	22.1
F4/80	1,274	86.3	19.1
CD11b	2	0.1	0.0

Cox2 MKO BMDM
D6: 86% F4/80

<u>Supplemental Figure 8</u> Bone marrow cells differentiate to F4/80+ macrophages after 6 days treatment with MCSF. Bone marrow was isolated from a *Cox2* MKO mouse and cultured for six days in the presence of 25 ng/ml rMCSF. After six days, living cells were FACS analyzed for expression of F4/80. In this instance, 86% of cells were F4/80+.

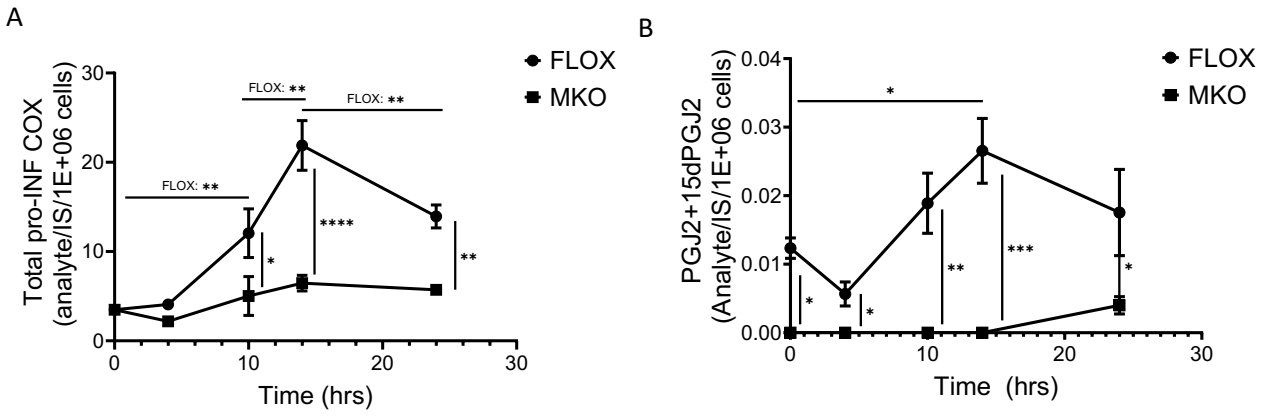

<u>Supplemental Figure 9.</u> ***Cox2*** **MKO suppresses the levels of COX metabolites including 15d-PGJ2 in LPS-activated BMDM.** BMDM were isolated from FLOX and *Cox2* MKO mice and activated with LPS (25 ng/ml). At various time points, lysate was collected, lipids were extracted, and the levels of COX inflammatory mediators was determined by LC-MS/MS. Consistent with the loss of myeloid *Cox2*, total COX pro-inflammatory mediators (**A**) were significantly suppressed from 10 hrs. The NFkB negative regulators PGJ2 + 15dPGJ2 were also significantly suppressed by *Cox2* MKO at all time points (**B**). (*Statistics*. Two-way ANOVA with Tukey's multiple comparisons test and adjusted p-values.)

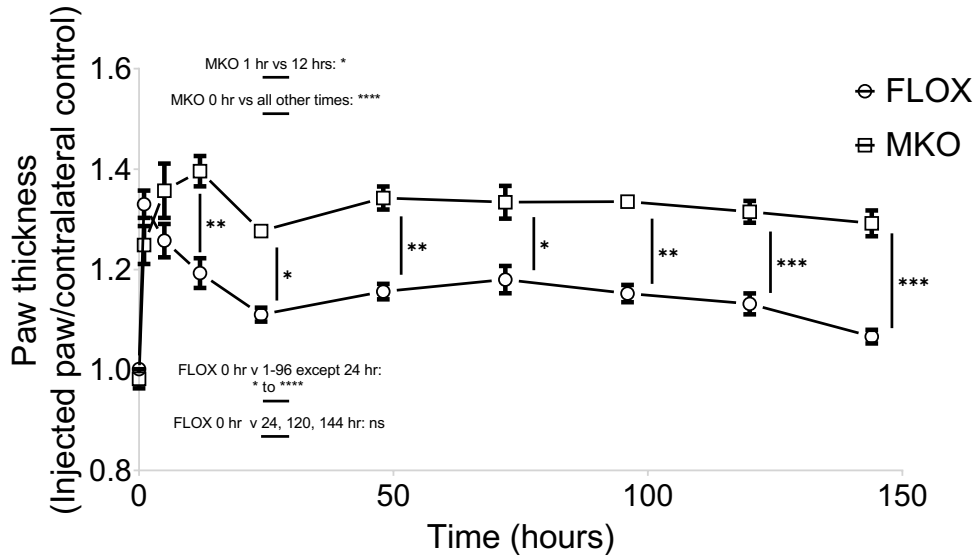

<u>Supplemental Figure 10.</u> *Cox2* MKO increases inflammation while delaying resolution in the carrageenan hind paw model. (*, $p < 0.05$; **, $p < 0.01$; ***, $p < 0.001$; ****, $p < 0.0001$) The hind paws of *Cox2* MKO (MKO) and FLOX mice were injected with carrageenan, and paw edema was determined as a marker of inflammation (n = 4). The initial peak of swelling was delayed in *Cox2* MKO compared to FLOX (12 vs 1 hr) and remained greater than FLOX across all time points from 12 hours. Paw swelling in FLOX mice was not significantly different than 0 hr baseline from 120 hrs. (*Statistics*: repeated measures two-way ANOVA with Tukey's multiple comparisons test and adjusted p-values.)

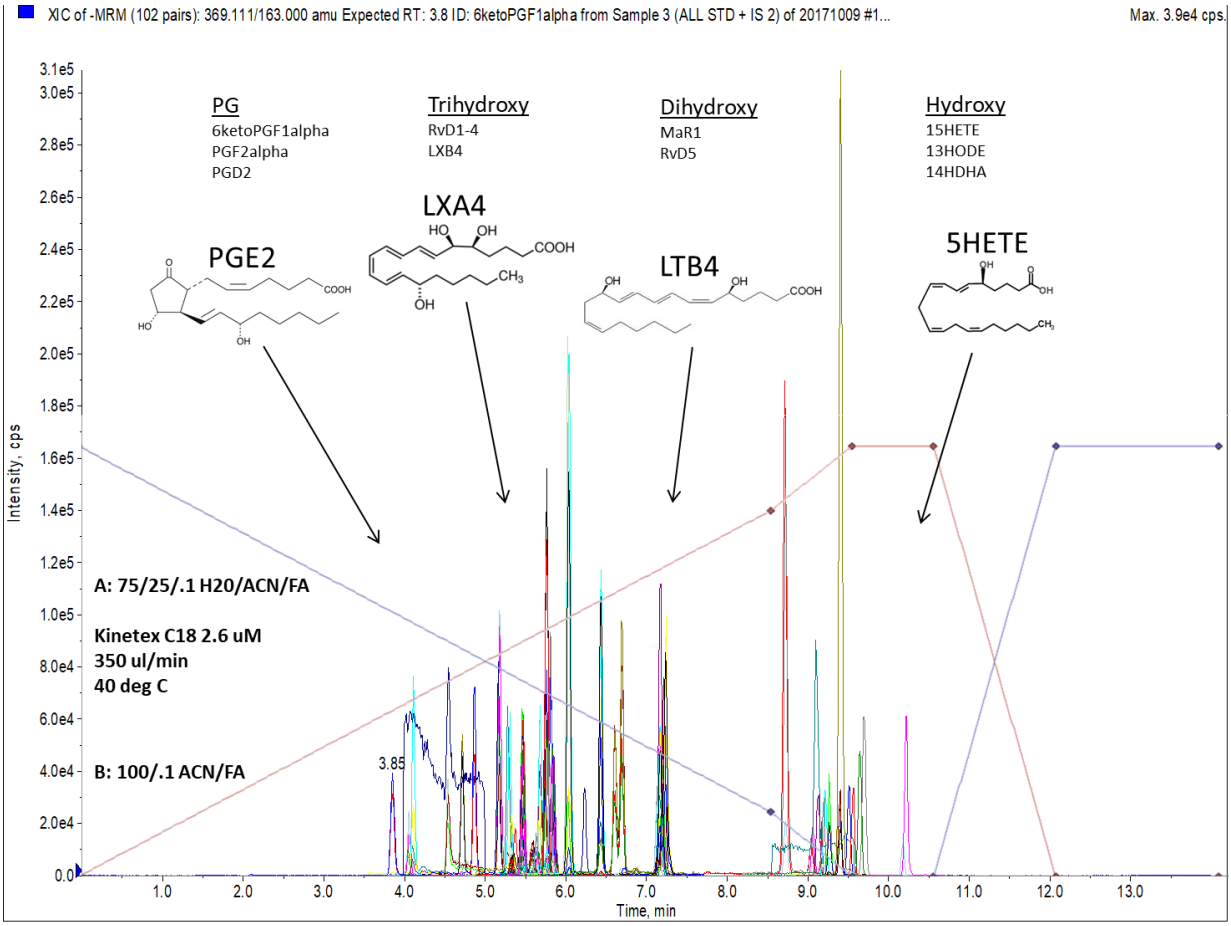

<u>Supplemental Figure 11.</u> Liquid chromatography provides good peak resolution and separation of all lipid analytes measured in this study. The complete chromatogram of all analytes of the lipid inflammatory mediator panel is given herein. The LC method is overlaid on the elution pattern, and examples of classes of compounds eluted in the distinct phases of the method are detailed. Sterically hindered and hydrophilic compounds are eluted first, with more hydrophobic compounds requiring increasing strength of the elution solvent to be pushed off the column.

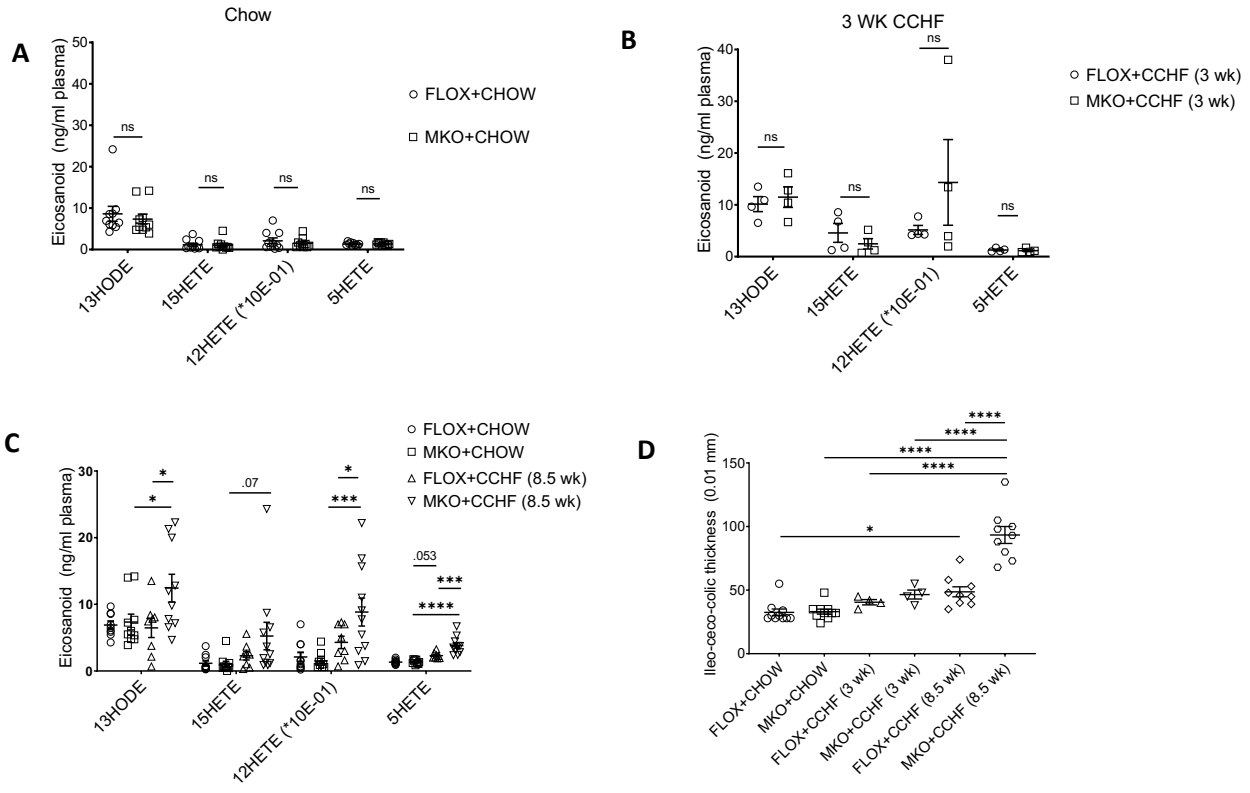

<u>Supplemental Figure 12.</u> Differential plasma levels of pro-inflammatory eicosanoids in *Cox2* MKO + CCHF-fed mice are correlated with the degree of intestinal inflammation. (*, $p < 0.05$; **, $p < 0.01$; ***, $p < 0.001$; ****, $p < 0.0001$) In an independent study, the levels of several pro-inflammatory lipoxygenase mediators in the plasmas of both MKO and FLOX mice were determined by LCMSMS following liquid-liquid extraction at chow diet baseline (**A**) and after 3 (**B**) and 8.5 weeks (**C**) of CCHF diet. Intestinal inflammation was measured as thickness of the ileo-ceco-colic junctions of the mice from A-C (**D**). Pro-inflammatory eicosanoid levels did not differ at baseline and after 3 weeks CCHF (A-B), while by 8.5 weeks MKO + CCHF mice exhibited significantly higher levels of these signals than both FLOX + CCHF and MKO + CHOW mice (C). This differential expression correlated with the emergence of severe ileo-ceco-colic thickening in MKO mice by 8.5 weeks (D). (*Statistics.* (A-B): Multiple Student's t-tests with Holm-Sidak correction for multiple tests and adjusted p-values. (C): For each analyte, two-way ANOVA with Tukey's multiple comparisons test and adjusted p-values. (D): one-way ANOVA with Tukey's multiple comparisons test and adjusted p-values.)

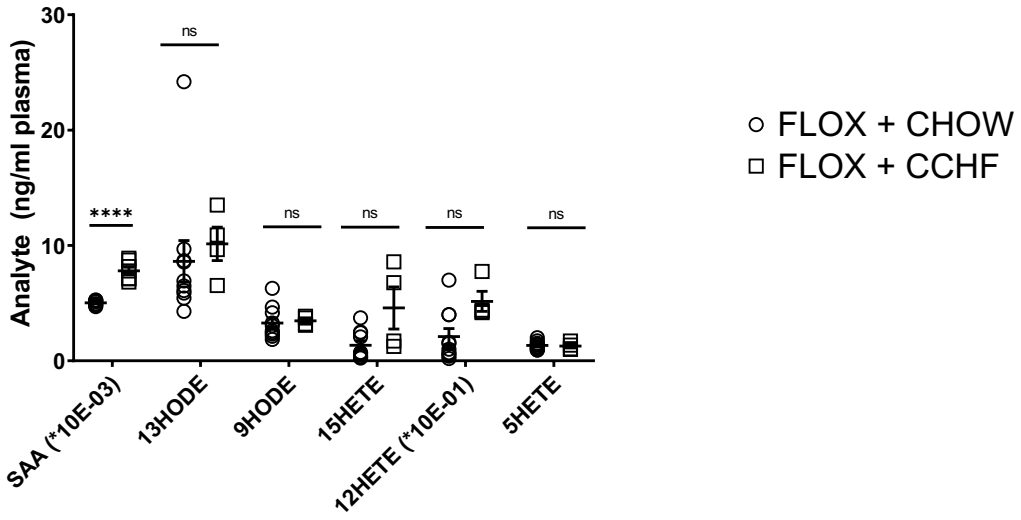

<u>Supplemental Figure 13.</u> Increase in SAA levels in FLOX + CCHF mice is not sufficient to elevate plasma lipid pro-inflammatory mediators. (****, $p < 0.0001$) FLOX mice were fed chow or CCHF diet for 3 weeks and both the systemic inflammation marker SAA as well as pro-inflammatory eicosanoids were determined in plasma, by ELISA and LC-MS/MS respectively. While FLOX mice exhibited a significant increase in SAA, none of the pro-inflammatory eicosanoids was significantly elevated. (*Statistics*. Multiple Student's t-tests with Holm-Sidak correction for multiple tests and adjusted p-values.)

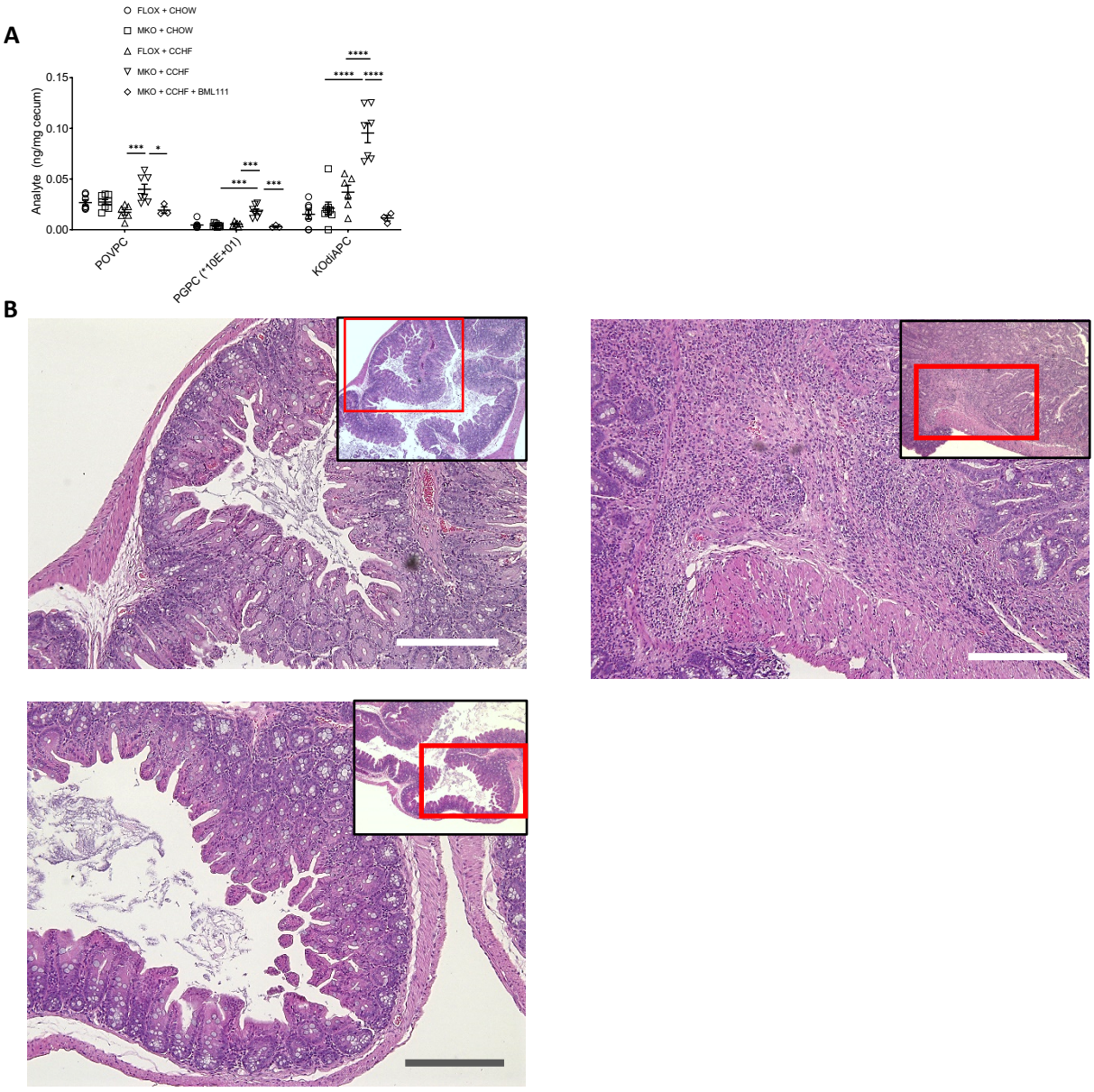

<u>Supplemental Figure 14.</u> The stable lipoxin A4 analog BML111 inhibits the development of intestinal inflammation in CCHF-fed *Cox2* MKO mice. (*, $p < 0.05$; ** $p < 0.01$; *** $p < 0.001$; ****, $p < 0.0001$) MKO and FLOX mice were fed chow or CCHF diet for 8.5 weeks prior to sacrifice (n = 10/group). Additional MKO mice (n = 9) on CCHF diet were injected i.p. twice weekly with the stable lipoxin analog BML111 (2 mg/kg) for the entire 8.5 weeks. Thicknesses of the ileo-ceco-colic junctions of all mice were determined, and ceca from some mice were assessed histologically (see Figure 2). Oxidized PAPC levels in additional ceca were determined by LC-MS/MS and compared to untreated controls (n = 3 and 7 per group) (**A**). Representative images FLOX + CCHF (upper *left*) and MKO + CCHF mice without (*upper right*) and with (*bottom left*) BML111 treatment (scale bar = 250 um) (**B**). (*Statistics*. One-way ANOVA with Tukey's multiple comparisons test and adjusted p-values.) (<u>Note</u>: Panel B *upper left* reproduces that in Supplemental Figure 5B *left*. The earlier representative image of the effect of CCHF on FLOX is from the above experiment; the panels are equally representative in both contexts.)

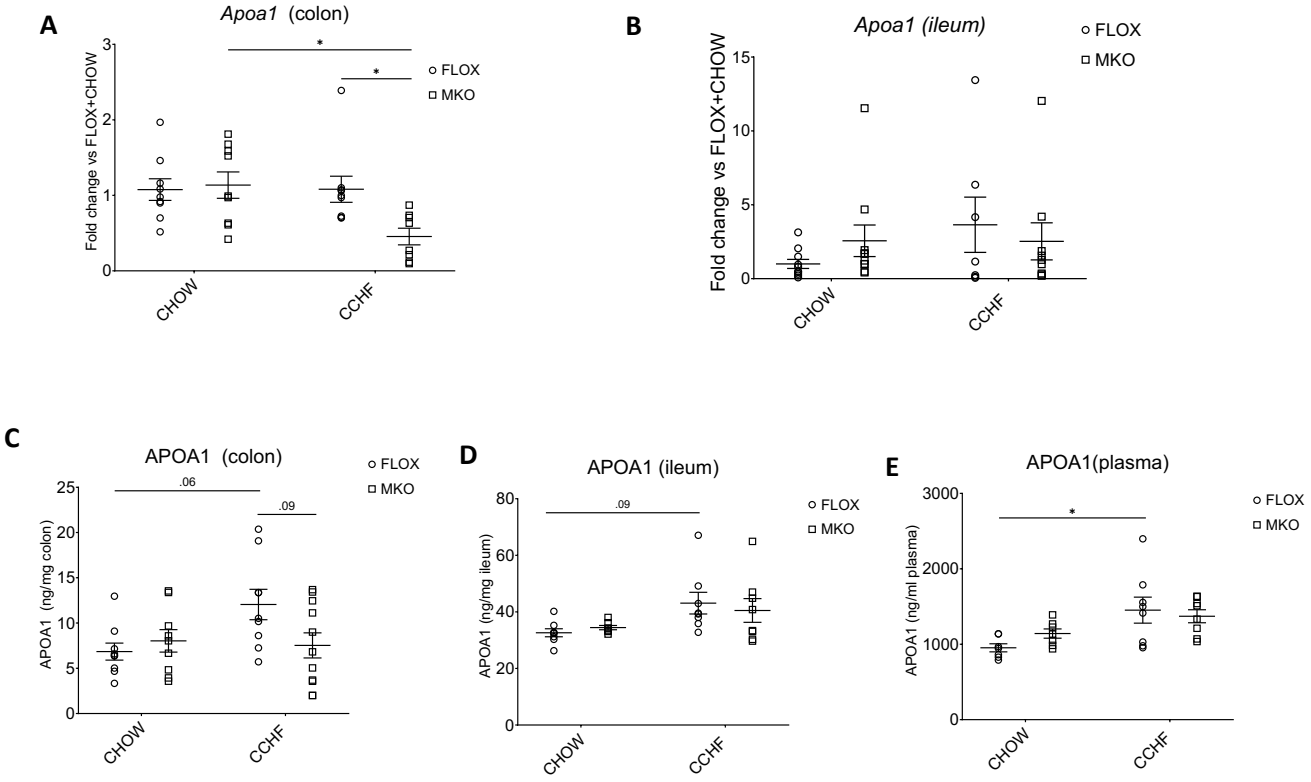

<u>Supplemental Figure 15.</u> *Apoa1* level is suppressed in the proximal colon of *Cox2* MKO + CCHF mice. **(*, $p < 0.05$)** *Apoa1* gene expression was determined by qPCR in the proximal colon (**A**) and the terminal ileum (**B**) of MKO and FLOX mice fed either chow or CCHF diet for 8.5 weeks. APOA1 protein levels were determined by ELISA in proximal colon (**C**), terminal ileum (**D**), and plasma (**E**) (n = 10/group). CCHF diet significantly suppressed *Apoa1* gene expression in the proximal colon of MKO mice, while protein levels in MKO + CCHF trended lower compared to FLOX + CCHF mice. By contrast, CCHF diet significantly increased APOA1 protein in plasma of FLOX mice. (*Statistics*. Two-way ANOVA with Tukey's multiple comparisons test and adjusted p-values.)

MKO + CCHF only

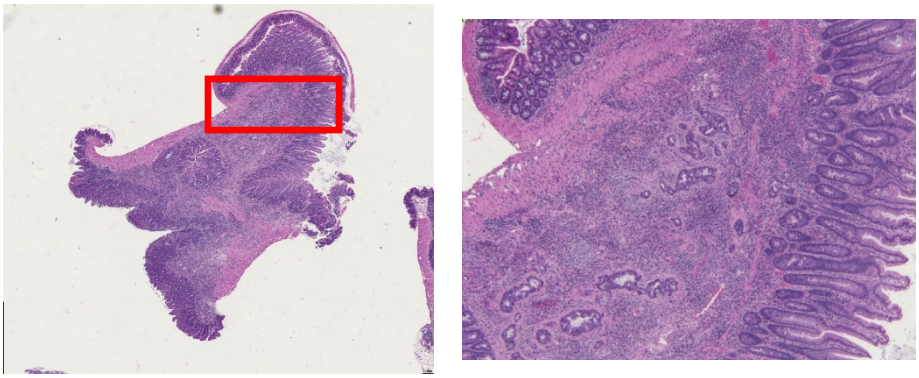

MKO + CCHF + Tg6F
(5 wk)

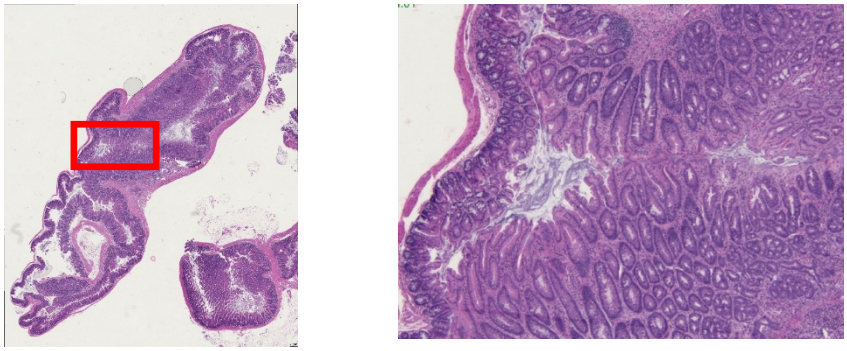

MKO + CCHF + Tg6F (10 wk)

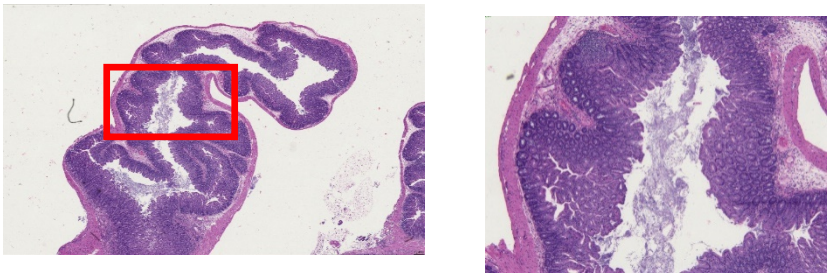

<u>Supplemental Figure 16.</u> Tg6F protects against intestinal inflammation in *Cox2* MKO mice on CCHF diet. *Cox2* MKO mice were challenged with CCHF for 10 weeks. Tg6F therapy was administered for either the full 10 weeks or the last 5 weeks of dietary challenge (20 mice/group). Both early and late onset therapy inhibited the progression of disease, as seen here H&E images from representative mice.

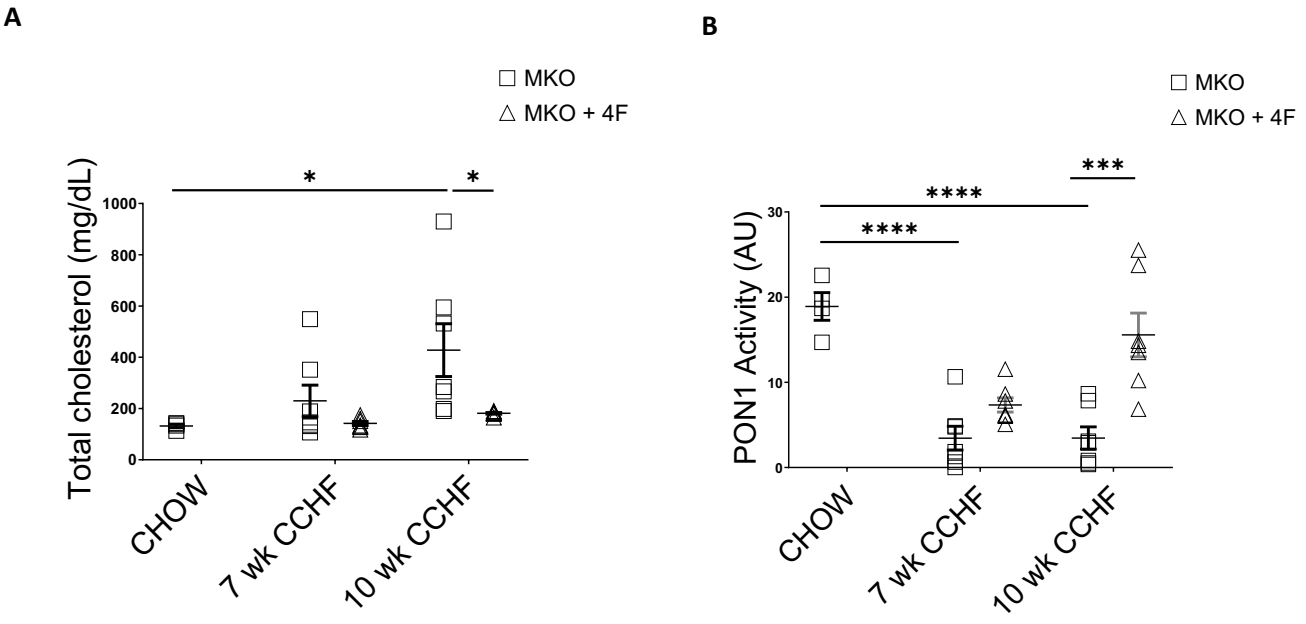

<u>Supplemental Figure 17.</u> 4F improves plasma total cholesterol and PON1 activity. (*, $p < 0.05$; ***, $p < 0.001$; ; ****, $p < 0.0001$) MKO mice were fed chow (n = 4) or CCHF diet with and without oral D-4F (500 ug/ml drinking water) (n = 6-7/group) for both 7 and 10 weeks. 4F therapy significantly reduced plasma total cholesterol by 10 weeks (**A**). The activity of PON1 (PON), an antioxidant enzyme associated with HDL whose activity is degraded by oxidative stress, was also significantly increased (**B**). (*Statistics*: one-way ANOVA with Tukey's multiple comparisons test and adjusted p-values.)

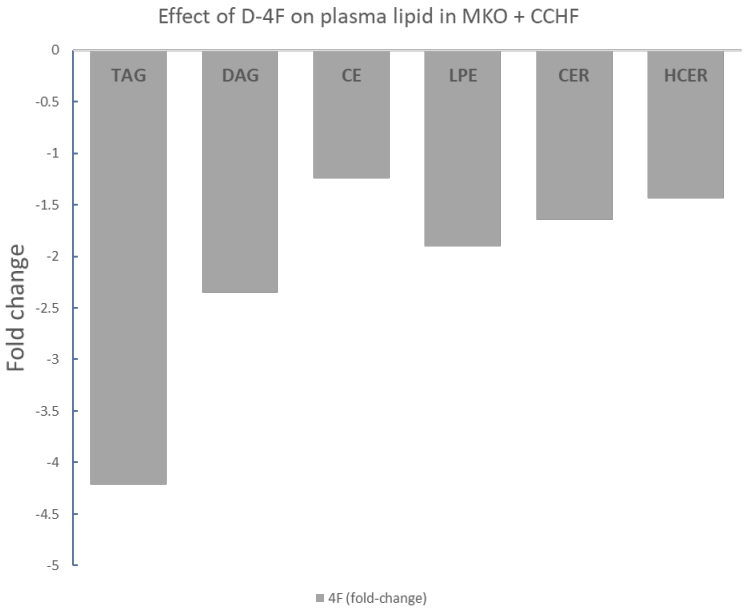

	Fold change	p-value
TAG	-4.216	0.000001
DAG	-2.356	0.0052
CE	-1.243	0.0002
LPE	-1.9	0.0002
CER	-1.649	0.0294
HCER	-1.437	0.0145
PE	-1.835	0.0609
PC	-1.756	0.2384
LPC	-1.241	0.6381
SM	-1.179	0.3065
FFA	1.2049	0.3703
LCER	ND	
DCER	ND	

<u>Supplemental Figure 18.</u> 4F therapy lowered broad classes of plasma lipids in *Cox2* MKO mice challenged with CCHF. MKO mice were fed CCHF for 8.5 weeks and the effect of 4F on broad classes of plasma lipids was determined on SCIEX's Lididyzer platform. Prior to correction for multiple t-tests, 4F significantly reduced total triacyglycerols (TAG) , diacylglycerols (DAG), cholesterol esters (CE) and lyso-phosphatidylethanolamines (LPE) ceramides (CER), and hexosylceramides (HCER). Following Holm-Sidak correction, TAG, DAG, CD, and LPE remained significantly reduced. (*Statistics*. Student's t-tests with Holm-Sidak correction for multiple tests.)

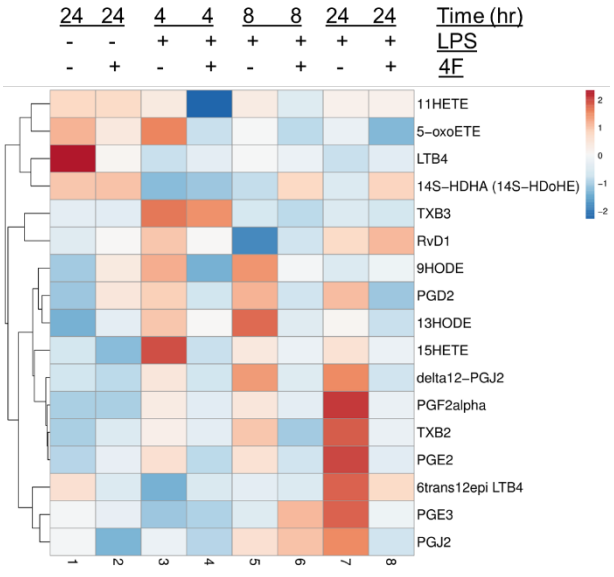

<u>Supplemental Figure 19.</u> 4F lowers the level of LPS-induced prostanoids in human THP-1 macrophages. LPS-activated THP-1 macrophages were treated with 4F up to 24 hrs. The levels of eicosanoids and docosanoids in cell lysate were determined by LC-MS/MS. 4F inhibited the LPS-dependent induction of prostanoids.

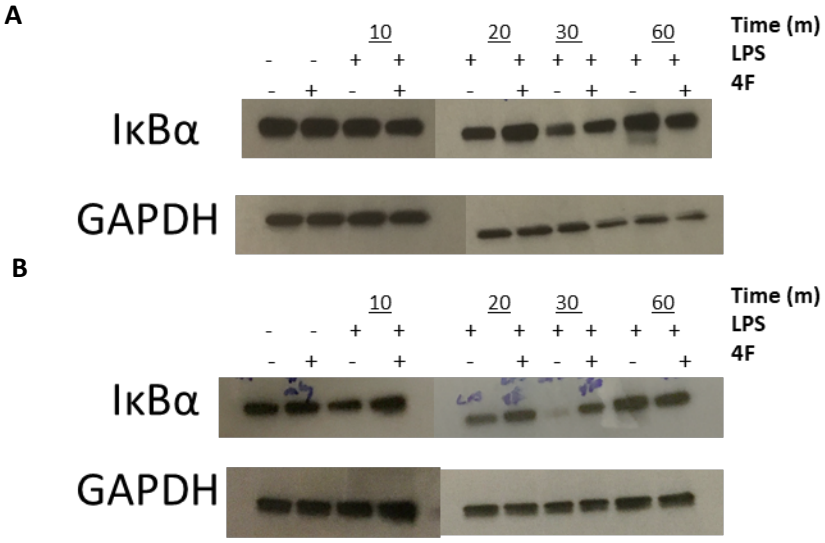

Supplemental Figure 20. 4F inhibits LPS-dependent degradation of IκBα (additional western blots). We treated THP1 macrophages with LPS and 4F across 60 minutes in two additional experiments and determined both IκBα and GAPDH by western blot (**A-B**) (cf. Figure 6B).

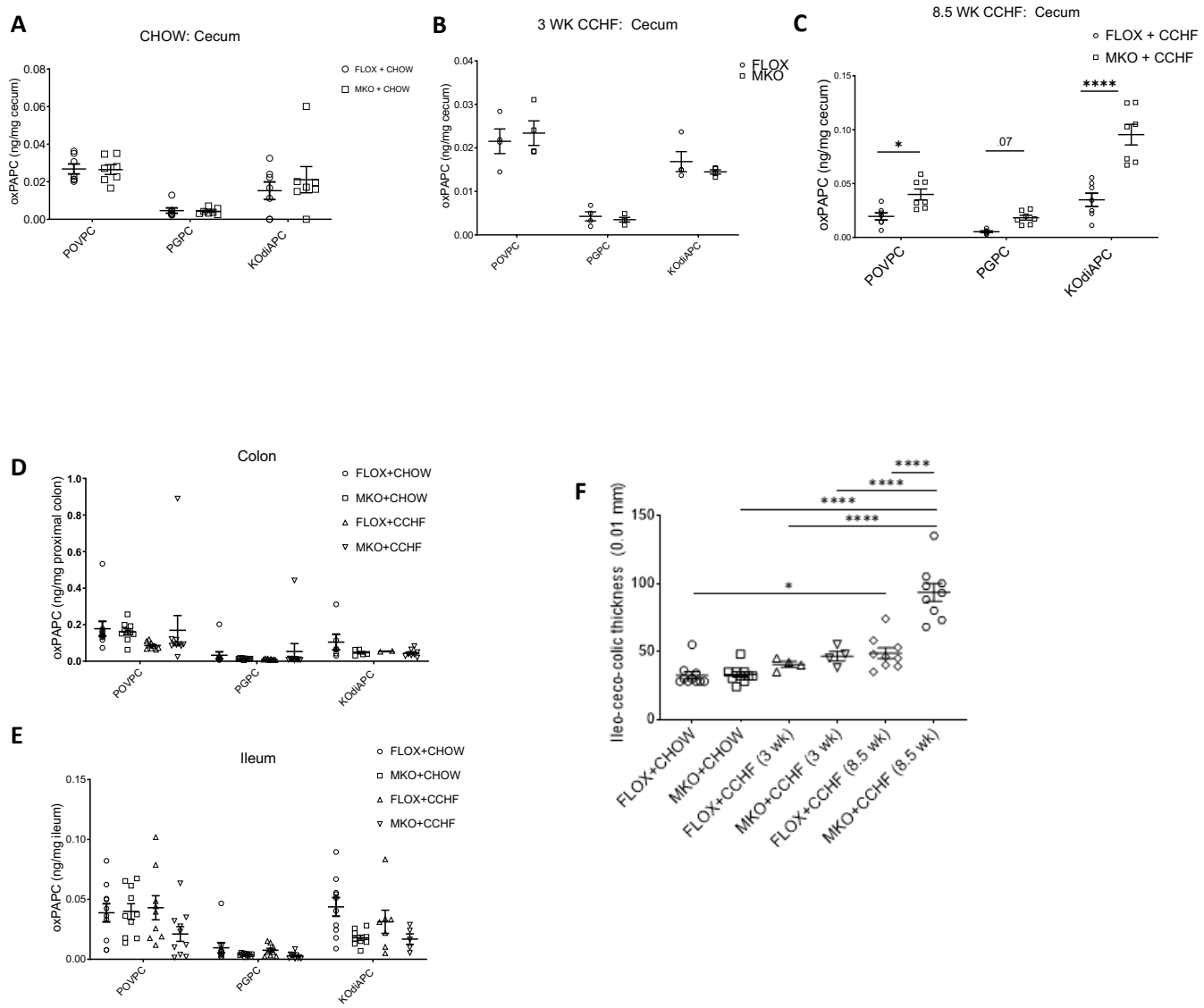

<u>Supplemental Figure 21.</u> Elevated oxPAPC levels in the intestine of *Cox2* MKO mice are associated with advanced intestinal inflammation. MKO and FLOX mice were fed chow or CCHF for 3 and 8.5 weeks. OxPAPC species were determined in the ceca of the mice at all three time points (**A-C**) (n = 7/group), as well as in the proximal colons and terminal ilea of FLOX and MKO mice after 8.5 weeks CCHF diet (**D-E**) (n = 10/group). Intestinal inflammation was measured as thickness of the ileo-ceco-colic junctions of these mice (**F**) (n = 10/group). We observed that all significant increases in oxPAPC species were localized to the ceca, were caused by 8.5 wk CCHF and, and were associated with advanced intestinal inflammation. (*Statistics*. (A-C): Multiple Student's t-tests with Holm-Sidak correction for multiple tests and adjusted p-values. (D-E): For each analyte, two-way ANOVA and Tukey's multiple comparison test and adjusted p-values. (F): One-way ANOVA with Tukey's multiple comparisons test and adjusted p-values.) (<u>Note</u>: (F) reproduces SFig 12D, on the grounds that we measured both eicosanoids and oxPAPC in the same mice.)

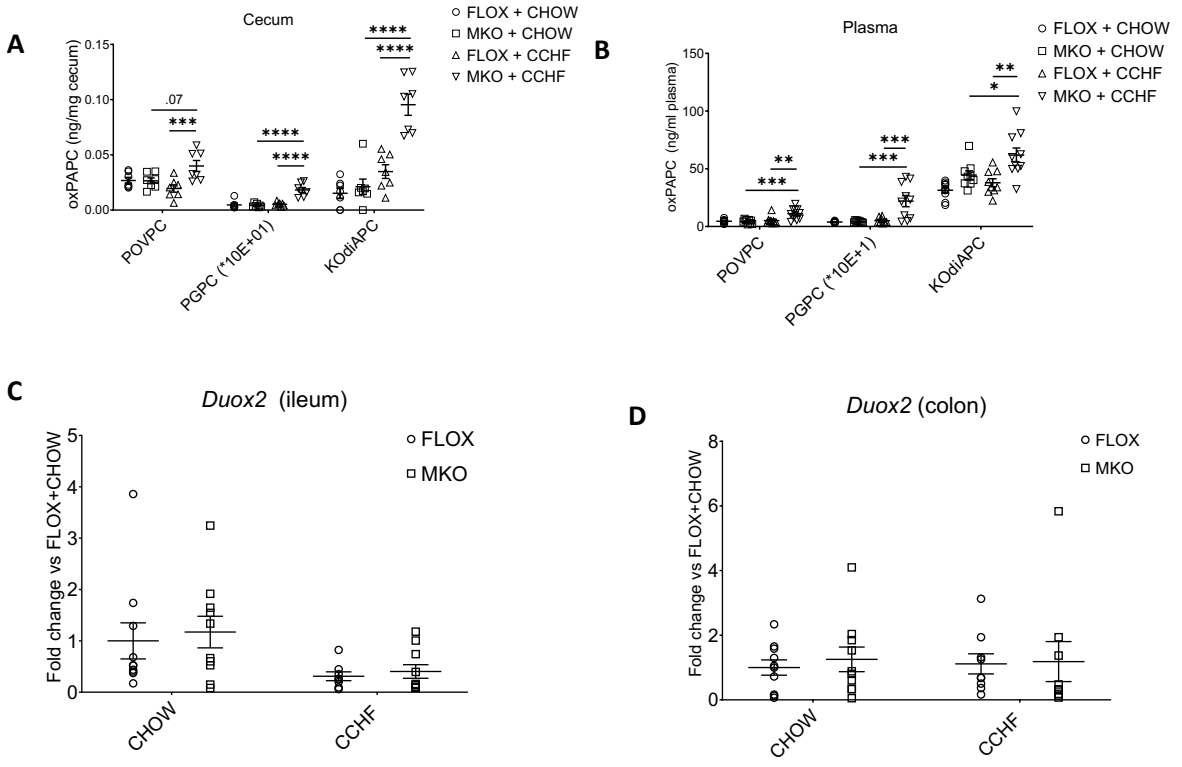

<u>Supplemental Figure 22.</u> CCHF diet increases the level of oxidized PAPC products in both the ceca and plasma of *Cox2* MKO mice, but independently of changes in *Duox*2 expression in both the terminal ileum and proximal colon. (*, $p < 0.05$; **, $p < 0.01$; ***, $p < 0.001$; ****, $p < 0.0001$) MKO and FLOX mice were fed chow or CCHF for 8.5 weeks. The oxidized PAPC products POVPC, PGPC, and KOdiAPC were measured using LC-MS/MS in both the ceca (**A**) (n = 7/group) and plasmas (**B**) (n = 10/group) of these mice. Both MKO and CCHF significantly increased all three oxidized PAPC products in the ceca and plasma of CCHF-fed and MKO mice, respectively. However, expression of dual oxidase 2 (*Duox2*)—a gene encoding for an enzyme in the digestive tract partially responsible for the production of hydrogen peroxide—was not increased in either the terminal ilea (**C**) or proximal colons (**D**) of MKO + CCHF-fed mice. (*Statistics*. (A-B): For each analyte, two-way ANOVA and Tukey's multiple comparisons test with adjusted p-values. (C-D): Two-way ANOVA with Tukey's multiple comparisons test with adjusted p-values.) (<u>Note</u>: (A-B) reproduce Figures 7A-B in order to aid the comparison between oxPAPC levels and *Duox2* expression.)

KD: 4F and 15HETE

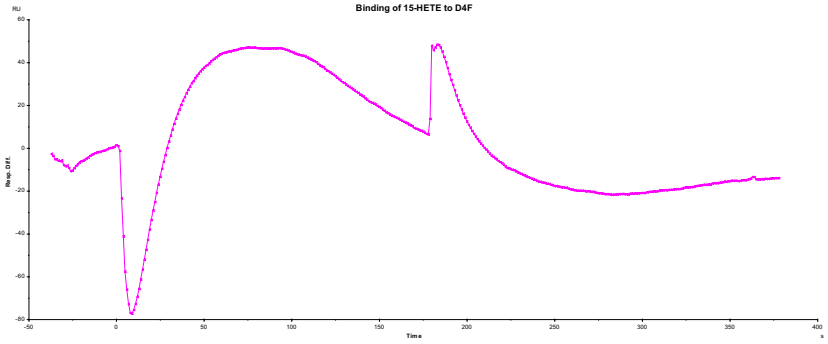

10 ng/ml 15-HETE to D4F

	ka (1/Ms)	kd (1/s)	Rmax (RU)	RI (RU)	Conc of analyte	KA (1/M)	**KD (M)**	Req (RU)	kobs (1/s)
10ng/ml 15-HETE to D4F	9.64e5	0.0321	286	-95	31.25n	3e7	**3.33e-8**	139	0.0622

KD: 4F and cholate

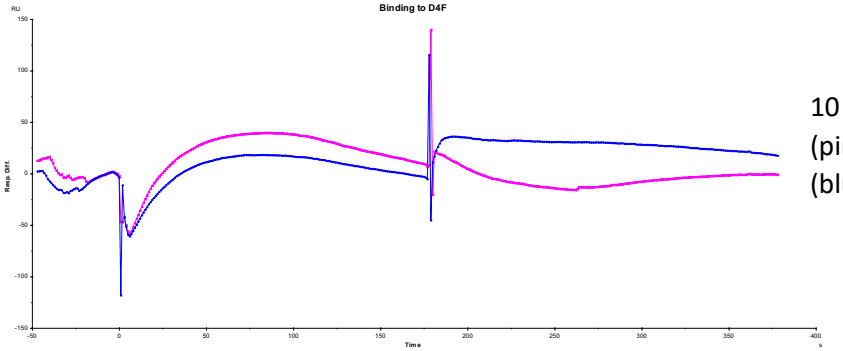

10 ug/ml Na cholate (pink) and deoxycholate (blue) to D4F

	ka (1/Ms)	kd (1/s)	Rmax (RU)	RI (RU)	Conc of analyte	KA (1/M)	**KD (M)**	Req (RU)	kobs (1/s)
10µg/ml Na Cholate to D4F	261	0.0426	834	-61.3	23226n	6.13e3	**1.63e-4**	104	0.0487

<u>Supplemental Figure 23.</u> 4F binds to cholate with comparatively low affinity. The binding affinity between 4F and cholate was determined by surface plasmon resonance. The high-binding 15 HETE was used as a positive control. In this study, 15HETE (KD = 30 nM) is approximately 30,000 fold more avid for 4F than cholate (KD = 160 uM).

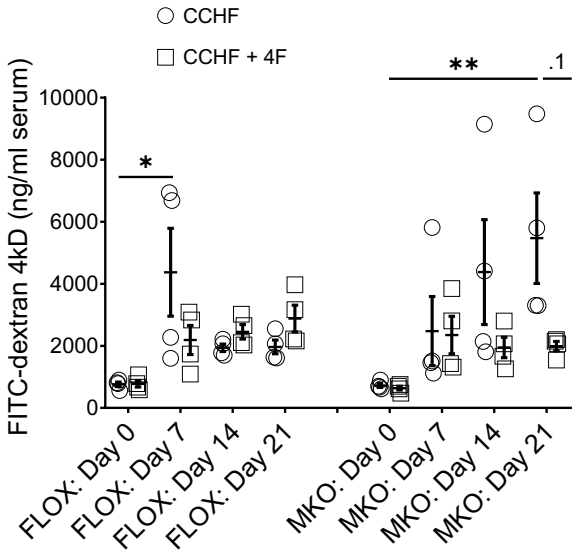

<u>Supplemental Figure 24.</u> 4F does not inhibit the initial CCHF-dependent increase in barrier permeability in either *Cox2* MKO or FLOX mice. (*, $p < 0.05$; **, $p < 0.01$) Both MKO and FLOX mice were fed CCHF diet with and without oral D-4F (500 ug/ml drinking water) (n = 4/group) for 21 days. Both at baseline and again after 7, 14, and 21 days, mice were water fasted for 4 hours; gavaged with FITC-dextran 4 kD (440 mg/kg); and bled retro-orbitally after 4 hours. The amount of FITC present in serum was determined. While CCHF significantly increased barrier permeability in both MKO and FLOX mice, 4F itself did not significantly inhibit this increase. At 21 days, however, there was a trend towards protection by 4F in MKO + CCHF mice ($p = 0.1$). (*Statistics*. For each of FLOX and MKO, two-way ANOVA with Tukey's multiple comparisons test and adjusted p-values.)

Supplemental Tables

Supplemental Table 1. Bioactive lipids, degradation products, and pathway markers determined by LC-MS/MS. All bioactive lipids, degradation products, and pathways markers analyzed by the LC-MS/MS method explained in the Supplemental Methods are listed herein. The particular analytes, their fatty acid precursors, their statuses (bioactive, pathway marker, degradation product), and their functions (pro or anti-inflammatory or inflammation resolving, or both pro- and anti-inflammatory) are detailed (see references 1-6).

Supplemental Table 2. Complete lipid panel with complete MS settings, assigned internal standards, and LC retention times. This table contains all of the optimized MS/MS settings for each analyte, together with the internal standards assigned to each lipid of interest listed in Supplementary Table 1. Isobaric compounds share a color. For compounds of the same color, specificity is generated by either unique fragment ions or by sufficient chromatographic separation. An example of an assignment of internal standards to two analytes is given.

Supplemental Table 3. Validation of LC-MS/MS method. Lower limit of detection (LLOD), lower limit of quantitation (LLOQ), upper limit of quantitation (ULOQ), and linearity of response are detailed for each of the analytes of interest in this method. A representative standard curve is provided.

Supplemental Table 4. **Precision of extractions from intestinal tissue and plasma.** Precision was determined for our sample preparation methods for intestinal tissue and plasma, with respect to all biologically available analytes within each matrix, as described in the Supplemental Methods. Precision is here reported as CV (%).

Supplemental Table 5. **Precision and extraction efficiency of internal standards in intestinal tissue and plasma.** Precision with respect to the area under the curve for each internal standard in both intestinal tissue and plasma was determined and reported as CV (%). Extraction efficiency for each internal standard was determined as the ratio of the recovery of 10 ng/ml IS from each matrix to the signal intensity of 10 ng/ml of each internal standard in methanol.

Supplemental Table 6. Effect of *Cox2* MKO, CCHF, and 4F on lipid inflammatory mediators in ileo-ceco-colic junctions of mice. *Cox2* MKO and FLOX mice were fed with CCHF diet for 8.5 weeks with and without D-4F (500 μg/ml drinking water). Lipid inflammatory mediator levels were determined in the ileo-ceco-colic junctions of these mice by LC-MS/MS.

Supplemental Table 7. Effect of *Cox2* MKO, CCHF, and 4F on lipid inflammatory mediators in plasma of mice. *Cox2* MKO and FLOX mice were fed with CCHF diet for 8.5 weeks with and without D-4F (500 μg/ml drinking water). Lipid inflammatory mediator levels were determined in the plasmas of these mice by LC-MS/MS.

Supplemental Tables 8-10. Application of Benjamini-Hochberg procedure to lipidomic data sets. Benjamini-Hochberg procedure for controlling FDR was applied to the 3 separate lipidomic data sets: *Cox2*MKO/CCHF intestine (Supplemental Table 6); *Cox2*MKO/CCHF plasma (Supplemental Table 7); PAC *Il10* intestine (Supplemental Table 11). For each analyte in a data set, statistical analysis of the multiple groups was initially performed by one-way ANOVA. Benjamini-Hochberg procedure was then applied to these p-values, with the FDR set at level $\alpha = 0.05$.

<u>Supplemental Tables 11-12</u>. The effect of oral D-4F on lipid inflammatory mediators in PAC *Il10* model of colitis. The effect of D-4F (500 µg/ml drinking water) on lipid inflammatory mediator levels in the PAC *Il10* model was determined by LC-MS/MS in the colons (Supplemental Table 11) and plasmas (Supplemental Table 12) of these mice.

Supplemental Table 1

Analyte	Precursor	Status	Function
COX			
Anti-INF COX			
PGJ2	AA, PGD2	nonezymatic metabolite of PGD2, **unstable**	inhibit platelet aggregation; *PGD2, 15dPGJ2 marker*
Δ12-PGJ2	AA, PGD2, PGJ2	bioactive, *PGD2/J2 marker*	Anti-INF: PPARgamma agonist; *PGD2/J2/15dPGJ2 marker*
15-deoxy-Δ12,14-PGJ2	AA, PGJ2	bioactive	Anti-INF: negative regulator of NFkB, PPARgamma agonist (PPARgamma reduces INF response of endo cells; increase PON1), Nrf2 activator
13-oxo-DHA	DHA	bioactive	Anti-INF: negative regulator of NFkB, PPARgamma agonist
13-oxo-DPA	DPA	bioactive	Anti-INF: negative regulator of NFkB, PPARgamma agonist
Pro-INF and pro-RES COX			
PGE2	AA	bioactive	Pro-INF: vascular leakage; pro-RES: class-switching
15ketoPGE2	AA, PGE2	*PGE2 marker, 15hydroxyPGDH product*	*PGE2 marker*
13,14-dihydro-15keto-PGE2	AA, PGE2	*PGE2 marker, 15hydroxyPGDH product*	*PGE2 marker*
PGD2	AA	bioactive	Pro-INF: PMN chemotaxis through DP1 DP2; pro-RES: class-switching; anti-INF: Nrf2 activator
13,14-dihydro-15keto-PGD2	AA, PGD2	*PGD2 marker, 15hydroxyPGDH product*	*PGD2 marker*
Further COX products (larely pro-INF)			
[PGI2]	AA	[bioactive but unstable]	Pro-INF: vasodilation
6ketoPGF1alpha	AA, PGI2	*hydrolysis product of PGI2, plasma*	*PGI2 marker*
PGF2alpha	AA	bioactive, **unstable**	Pro-INF: RA, ath
13,14-dihydro-15-keto Prostaglandin F2α	AA, PGF2alpha	*product of PGF2alpha, plasma*	*PGF2alpha marker*
[TXA2]	AA	[bioactive but unstable]	Pro-INF: microvascular constriction, PMN adherence (overall:vasoconstriction and platelet aggregation)
TXB2	AA, TXA2	bioactive, *TXA2 product*	Pro-INF: PMN chemotaxis and adherence (maybe through TXA2)
11HETE	AA	*pathway marker (COX)*	*COX activity marker*
15HETE	AA	*Precursor; pathway marker (COX, 15LOX, LX)*	Anti-INF: LX precursor
PGE3	EPA	bioactive	Pro-INF: induce COX2 and IL6 in macrophage
TXB3	EPA	bioactive but less than TXA2/B2, *TXA3 product*	Pro-INF: induce COX2 and IL6 in macrophage

LOX			
Pro-INF LOX products			
LTB4	AA, LTA4	bioactive	Pro-INF: vascular leakage; leukocyte chemotaxis and adhesion
6trans12epi LTB4	AA, LTA4	*non-enzymatic hydrolysis product of LTA4*	*LT marker*
20-OH-LTB4	AA, LTB4	*LTB4 metabolite (LTB4 20 hydroxylase)*	*LTB4 marker*
LTC4	AA, LTA4	bioactive, *glutathione conjugate of LTA4*	Pro-INF: vascular permeability (macrophage product)
LTE4	AA, LTA4	*plasma marker of LTD4*	*LTD4 marker, plasma and urine*
5HETE	AA	*bioactive; pathway marker, 5LOX*	pro-INF: PMN chemotaxis and degranulation
12HETE	AA	bioactive	pro-INF: neutrophil chemotaxis and adhesion
15HETE	AA	*pathway marker, LX*	
5-oxoETE	AA,5HETE (dehydrogenase)	bioactive	pro-INF: PMN chemotaxis and degranulation
13HODE	LA	bioactive	pro-INF: PMN chemotaxis
9HODE	LA	bioactive	pro-INF: PMN chemotaxis
Pro-RES LOX products			
LXA4	AA; 15HETE[5LOX]; LTA4[15LOX]	bioactive	pro-RES and anti-INF: promote M1 to M2; NFkB negative regulator; inhibit neutrophil chemotaxis and adhesion
15epi-LXA4	AA; 15HETE[5LOX]; LTA4[15LOX]	bioactive	pro-RES and anti-INF: promote M1 to M2; NFkB negative regulator; inhibit neutrophil chemotaxis and adhesion
5,15-diHETE	AA; 5HETE[15LOX]	bioactive; *pathway marker, LX*;	*pathway marker, LX*; proINF: PMN degranulation and chemotaxis
LXB4	AA	bioactive	pro-RES and anti-INF: promote M1 to M2; NFkB negative regulator; inhibit neutrophil chemotaxis and adhesion
MaR--1	DHA;	bioactive	pro-RES; tissue regeneration; M1 to M2; inhibit neutrophil migration; increase efferocytosis
14S-HDHA (14S-HDoHE)	DHA	*pathway marker, MaR1; oxidation product*	*Mar1 marker*
RvD1	DHA[15LOX,5LOX]	bioactive	pro-RES: limit neutrophil infiltration
RvD2	DHA	bioactive	pro-RES: enhanace survival in sepsis; protect against colitis
RvD3	DHA	bioactive	pro-RES: limit leukocyte migration, enhance macrophage efferocytosis
RvD4	DHA	bioactive	
RvD5	DHA	bioactive	pro-RES: enhance bacterial containment and phagocytosis
17S-HDHA (17S-HDoHE)	DHA	*pathway marker, RvD PD*	*RvD and PD marker*
PDx (10S,17S-DiHDHA)	DHA	bioactive	pro-RES: inhibit neutrophil infiltration and platelet aggregation
RvE1	EPA	bioactive	pro-RES: reduce PMN infiltration; promote resolution in colitis model
18HEPE	EPA	*pathway marker, RvE*	*RvE marker*

Supplemental Table 2

COMPLETE LIPID PANEL: IS, RT, MS/MS

Analyte	Internal Standard	MW	RT	MS1	DP	EP	MS2-1	CE	CXP	MS2-2	CE	CXP
18HEPE	RvE1-d4	318.5	1.52	317.102	-90	-10	113	-22	-5	248.9	-10	-11
6ketoPGF1alpha	RvE1-d4	370.5	3.78	369.111	-145	-10	163	-36	-7	245.2	-36	-9
RvE1-d4		354.5	3.95	353.121	-120	-10	109.1	-26	-5	197.1	-24	-7
RvE1	**RvE1-d4**	350.5	3.98	349.12	-130	-10	107.1	-26	-5	161	-26	-5
TXB3	TXB2-d4	368.5	4.03	367.016	-110	-10	169.2	-24	-7	195.1	-16	-9
20-OH-LTB4	RvE1-d4	352.5	4.05	351.099	-100	-10	195.1	-24	-9	333.1	-22	-13
TXB2-d4		374.5	4.46	373.105	-135	-10	173.1	-22	-7	199.1	-18	-9
TXB2	**TXB2-d4**	370.5	4.48	369.074	-105	-10	169.1	-24	-7	195.2	-20	-7
PGE3	PGE2-d4	350.5	4.67	349.147	-80	-10	269.1	-22	-13	313.2	-16	-11
PGF2alpha	PGE2-d4	354.5	4.80	353.163	-145	-10	309.2	-26	-11	193.1	-34	-7
PGE2-d4		356.5	5.09	355.3	-95	-10	319.2	-18	-11	275.2	-24	-11
PGE2*	**PGE2-d4**	352.5	5.11	351.3	-100	-10	315.3	-17	-11.5	271.2	-24.4	-10
RvD3-d5		381.5	5.22	380.141	-140	-10	152.1	-26	-7	115.1	-26	-5
RvD3	**RvD3-d5**	376.5	5.25	375.022	-70	-10	147.1	-26	-7	103.1	-34	-5
LXB4	RvD3-d5	352.5	5.28	351.127	-120	-10	221.1	-22	-9	315.2	-20	-5
PGD2-d4		356.5	5.38	355.2	-95	-10	275.2	-24	-11	319.2	-16	-13
PGD2*	**PGD2-d4**	352.5	5.39	351.2	-65	-10	97	-40	-5	189.2	-26	-7
RvD2-d5		381.5	5.40	380.148	-95	-10	175.1	-32	-7	141	-22	-5
RvD2	**RvD2-d5**	376.5	5.41	375.101	-90	-10	175.1	-30	-7	141	-22	-7
LTC4-d5		630.8	5.44	629.116	-95	-10	272.1	-34	-11	142.9	-48	-7
LTC4	**LTC4-d5**	625.8	5.47	624.133	-100	-10	272.1	-30	-7	143.1	-42	-5
15ketoPGE2	PGE2-d4	350.5	5.61	349.159	-115	-10	331.1	-16	-5	235.1	-20	-9
LTE4	LTC4-d5	439.6	5.67	438.122	-100	-10	333.2	-24	-13	235.2	-28	-9
LXA4-d5		357.5	5.70	356.189	-95	-10	115.1	-20	-5	222.2	-28	-9
LXA 4	**LXA4-d5**	352.5	5.70	351.159	-90	-10	115	-20	-5	217.2	-28	-9
15epi-LXA4	LXA 4-d5	352.5	5.72	351.128	-95	-10	115	-20	-5	217.1	-28	-9
RvD1-d5		381.5	5.76	380.159	-100	-10	141	-20	-7	220.2	-30	-9
13,14-dihydro-15-keto PGF2α-d4		358.5	5.77	357.18	-180	-10	113.1	-36	-5	187.2	-36	-9
RvD1	**RvD1-d5**	376.5	5.78	375.002	-50	-10	103	-24	-3	140.9	-20	-5
13,14-dihydro-15-PGF2α	**13,14-dihydro-15-keto PGF2α-d4**	354.5	5.80	353.167	-130	-10	113	-38	-5	183.1	-36	-9
13,14-dihydro-15keto-PGE2	**13,14-dihydro-15-keto PGE2-d4**	352.5	5.98	351.164	-100	-10	333.2	-18	-13	175.1	-32	-7
13,14-dihydro-15-keto PGE2-d4		356.5	6.02	355.152	-100	-10	337.3	-18	-11	179.1	-32	-7
RvD4	RvD1-d5	376.5	6.18	375.021	-90	-10	103	-26	-5	101.1	-32	-5
13,14-dihydro-15keto-PGD2	13,14-dihydro-15-keto PGE2-d4	352.5	6.41	351.127	-110	-10	333.3	-16	-3	207	-26	-7
PGJ2	13,14-dihydro-15-keto PGE2-d4	334.5	6.55	333.123	-105	-10	315.1	-14	-11	189.2	-22	-7
Δ12-PGJ2	13,14-dihydro-15-keto PGE2-d4	334.5	6.64	333.144	-145	-10	315.1	-14	-13	271.2	-22	-11
MaR1-d5		365.5	7.06	364.202	-130	-10	123	-24	-5	93	-44	-9
MaR1-	**MaR1-d5**	360.5	7.11	359.124	-115	-10	93.1	-42	-5	123.1	-22	-19
PDx (10S,17S-DiHDHA)	MaR1-d5	360.5	7.12	359.119	-65	-10	153.1	-24	-5	93.1	-40	-11
6trans12epi LTB4	LTB4-d4	336.5	7.12	335.157	-145	-10	195.2	-22	-7	317.2	-20	-11
RvD5	LTB4-d4	360.5	7.14	359.104	-100	-10	199.1	-22	-9	140.9	-20	-5
LTB4-d4		340.5	7.16	339.181	-125	-10	197.1	-22	-9	321.1	-20	-13
LTB4	**LTB4-d4**	336.5	7.20	335.155	-115	-10	195.1	-20	-7	317.2	-20	-5
15d-PGJ2-d4		320.5	8.66	319.2	-130	-10	275.2	-20	-11	80	-88	-5
15-deoxy-Δ 12, 14-PGJ2	**15d-PGJ2-d4**	316.4	8.69	315.3	-130	-10	271.1	-20	-11	203.1	-30	-7
13HODE-d4		300.5	9.02	299.066	-220	-10	198	-28	-9			
13HODE	**13HODE-d4**	296.5	9.06	295.09	-180	-10	295.09	-28	-9			
9HODE	13HODE-d4	296.5	9.09	295.108	-145	-10	170.8	-26	-27			
15HETE d8		328.5	9.17	327.146	-150	-10	226	-18	-9			
15HETE	**15HETE d8**	328.5	9.23	319.063	-170	-10	219.1	-18	-9			
17S-HDHA (17S-HDoHE)	15HETE d8	344.5	9.24	343.147	-100	-10	281.2	-20	-11	245.1	-16	-9
14S-HDHA (14S-HDoHE)	15HETE d8	344.5	9.37	343.167	-115	-10	281.2	-18	-11	161.2	-20	-5
11HETE	12HETE-d8	320.5	9.38	319.148	-95	-10	167	-24	-7	149	-28	-23
12HETE-d8		328.5	9.47	327.117	-145	-10	184	-22	-5			
12HETE	**12HETE-d8**	320.5	9.53	319.039	-30	-10	178.8	-20	-5			
5HETE-d8		328.5	9.61	327.139	-145	-10	115.9	-24	-5			
5HETE	**5HETE-d8**	320.5	9.67	319.087	-160	-10	115	-20	-5			
5-oxo-ETE-d7		325.5	10.15	324.22	-120	-10	210.2	-26	-9	120	-18	-5
5-oxoETE	**5-oxo-ETE-d7**	318.5	10.2	317.154	-125	-10	113	-20	-5	203.2	-26	-9

39 ANALYTES
19 INTERNAL STANDARDS (IS)
--Either exact or class specific.
Examples given below.

Analyte	IS	MW	RT
PGF2alpha	PGE2-d4	354.5	4.80
PGE2-d4		356.5	5.09
PGE2*	**PGE2-d4**	352.5	5.11

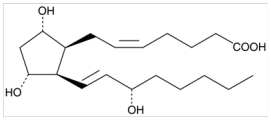

PGF2alpha

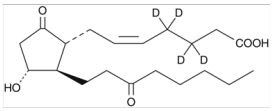

PGE2-d4

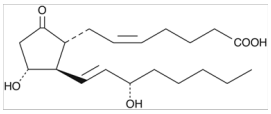

PGE2

Supplemental Table 3

Analyte	Internal S	MW	RT	MS1	LLOD (ng	LLOQ (ng	ULOQ (ng	Crv fit (r)
18-EPE	RvE1-d4	318.5	1.52	**317.102**	NA	NA	NA	NA
6ketoPGF	RvE1-d4	370.5	3.78	**369.111**	<0.078	0.15	>80	0.997
RvE1-d4		354.5	3.95	**353.121**				
RvE1	**RvE1-d4**	350.5	3.98	**349.12**	<0.078	0.31	>80	0.994
TXB3	TXB2-d4	368.5	4.03	**367.016**	0.078	0.625	>80	0.987
20-OH-LTE	RvE1-d4	352.5	4.05	**351.099**	<0.078	0.15	>80	0.995
TXB2-d4		374.5	4.46	**373.105**				
TXB2	**TXB2-d4**	370.5	4.48	**369.074**	<0.31	0.31	>80	0.99
PGE3	PGE2-d4	350.5	4.67	**349.147**	<0.15	0.15	>80	0.999
PGF2alph	PGE2-d4	354.5	4.80	**353.163**	<0.078	0.15	>80	0.997
PGE2-d4		356.5	5.09	**355.3**				
PGE2*	**PGE2-d4**	352.5	5.11	**351.3**	<0.078	0.15	>80	0.993
RvD3-d5		381.5	5.22	**380.141**				
RvD3	**RvD3-d5**	376.5	5.25	**375.022**	<0.078	0.15	>80	0.983
LXB4	RvD3-d5	352.5	5.28	**351.127**	<0.078	0.31	>80	0.99
PGD2-d4		356.5	5.38	**355.2**				
PGD2*	**PGD2-d4**	352.5	5.39	**351.2**	<0.078	0.15	>80	0.99
RvD2-d5		381.5	5.40	**380.148**				
RvD2	**RvD2-d5**	376.5	5.41	**375.101**	< .15	0.15	>80	0.996
LTC4-d5		630.8	5.44	**629.116**				
LTC4	**LTC4-d5**	625.8	5.47	**624.133**	<0.078	0.15	>80	0.997
15ketoPG	PGE2-d4	350.5	5.61	**349.159**	<0.078	0.31	>80	0.997
LTE4	LTC4-d5	439.6	5.67	**438.122**	<0.078	0.31	>80	0.983
LXA4-d5		357.5	5.70	**356.189**				
LXA4	**LXA4-d5**	352.5	5.70	**351.159**	<0.078	0.31	>80	0.99
15epi-LXA	LXA4-d5	352.5	5.72	**351.128**	<0.078	0.15	>80	0.998
RvD1-d5		381.5	5.76	**380.159**				
13,14-dihydro-15-ket		358.5	5.77	**357.18**				
RvD1	**RvD1-d5**	376.5	5.78	**375.002**	< .15	0.15	>80	0.998
13,14-dihy	**13,14-dihy**	354.5	5.80	**353.167**	<0.078	0.15	>80	0.995
13,14-dihy	**13,14-dihy**	352.5	5.98	**351.164**	<0.078	0.15	>80	0.993
13,14-dihydro-15-ket		356.5	6.02	**355.152**				
RvD4	RvD1-d5	376.5	6.18	**375.021**	<0.078	0.15	>80	0.99
13,14-dihy	13,14-dihy	352.5	6.41	**351.127**	<0.078	0.15	>80	0.99
PGJ2	13,14-dihy	334.5	6.55	**333.123**	<0.078	0.15	>80	0.99
Δ12-PGJ	13,14-dihy	334.5	6.64	**333.144**	< .15	0.15	>80	0.998
MaR1-d5		365.5	7.06	**364.202**				
MaR1-	**MaR1-d5**	360.5	7.11	**359.124**	0.078	0.31	>80	0.996
PDx (10S,	MaR1-d5	360.5	7.12	**359.119**	<0.078	0.15	>80	0.997
8trans12e	LTB4-d4	336.5	7.12	**335.157**	<0.078	0.15	>80	0.98
RvD5	LTB4-d4	360.5	7.14	**359.104**	<0.078	0.15	>80	0.99
LTB4-d4		340.5	7.16	**339.181**				
LTB4	**LTB4-d4**	336.5	7.20	**335.155**	<0.078	0.31	>80	0.99
15d-PGJ2-d4		320.5	8.66	**319.2**				
15-deoxy-Δ	**15d-PGJ2**	316.4	8.69	**315.3**	< .15	0.15	>80	0.998
13HODE-d4		300.5	9.02	**299.066**				
13HODE	**13HODE-d**	296.5	9.06	**295.09**	< .15	0.31	>80	0.994
9HODE	13HODE-d	296.5	9.09	**295.108**	<0.078	0.31	>80	0.991
15HETE-d8		328.5	9.17	**327.146**				
15-HETE	**15HETE-d8**	320.5	9.23	**319.063**	<0.078	0.31	>80	0.99
17S-HDHA	15HETE-d8	344.5	9.24	**343.147**	<0.078	0.15	>80	0.99
14S-HDHA	15HETE-d8	344.5	9.37	**343.167**	<0.078	0.31	>80	0.99
11HETE	12HETE-d8	320.5	9.38	**319.148**	< .15	0.31	>80	0.998
12HETE-d8		328.5	9.47	**327.117**				
12-HETE	**12HETE-d**	320.5	9.53	**319.039**				
5HETE-d8		328.5	9.61	**327.139**				
5HETE	**5HETE-d8**	328.5	9.67	**319.087**	<0.078	0.15	>80	0.995
5-oxo-ETE-d7		325.5	10.15	**324.22**				
5-oxoETE	**5-oxo-ETE**	318.5	10.2	**317.154**	<0.078	0.31	>80	0.98

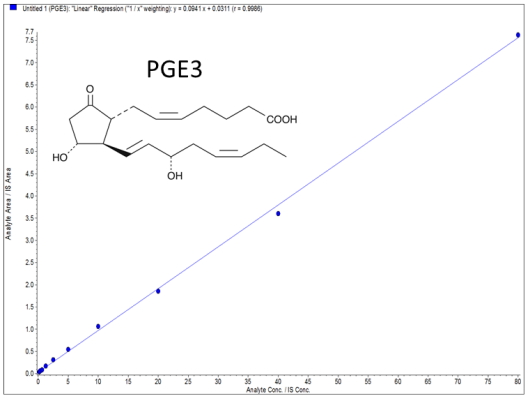

Analyte	IS	MW	RT	MS1	LLOD (ng/ml)	LLOQ (ng/ml)	ULOQ (ng/ml)	Crv fit (r)
PGE3	PGE2-d4	350.5	4.67	**349.147**	<0.078	0.15	>80	0.999

Supplemental Table 4

Tissue

Analyte	IS	CV(%)
6ketoPGF1alpha	RvE1-d4	8.93
RvE1	RvE1-d4	NA
TXB3	TXB2-d4	3.42
20-OH-LTB4	RvE1-d4	14.94
TXB2	TXB2-d4	4.24
PGE3	PGE2-d4	3.23
PGF2alpha	PGE2-d4	4.85
PGE2*	PGE2-d4	2.37
RvD3	RvD3-d5	NA
LXB4	RvD3-d5	12.08
PGD2*	PGD2-d4	4.04
RvD2	RvD2-d5	NA
LTC4	LTC4-d5	13.47
15ketoPGE2	PGE2-d4	**43.89**
LTE4	LTC4-d5	17.50
LXA4	LXA4-d5	18.07
15epi-LXA4	(No IS)	NA
RvD1	RvD1-d5	10.55
13,14-dihydro-15-PGF2α	13,14-dihydro-15-keto PGF2α-d4	6.14
13,14-dihydro-15keto-PGE2	13,14-dihydro-15-keto PGE2-d4	0.29
RvD4	RvD1-d5	NA
PGJ2	13,14-dihydro-15-keto PGE2-d4	11.59
13,14-dihydro-15keto-PGD2	13,14-dihydro-15-keto PGE2-d4	6.89
Δ12-PGJ2	13,14-dihydro-15-keto PGE2-d4	14.51
MaR1-	MaR1-d5	5.56
PDx (10S,17S-DiHDHA)	MaR1-d5	4.91
6trans12epi LTB4	LTB4-d4	13.29
RvD5	LTB4-d4	3.14
LTB4	LTB4-d4	2.94
15-deoxy-Δ12,14-PGJ2	15d-PGJ2-d4	15.96
13HODE	13HODE-d4	1.32
9HODE	13HODE-d4	3.01
17S-HDHA (17S-HDoHE)	15HETEd8	9.95
15HETE	15HETEd8	11.30
14S-HDHA (14S-HDoHE)	15HETEd8	4.94
11HETE	12HETE-d8	4.98
12HETE	12HETE-d8	1.26
5HETE	5HETE-d8	6.30
5-oxoETE	5-oxo-ETE-d7	14.47

Plasma

	CV (%)	Extraction efficiency of IS (%)
11HETE	2.92	81.73
12HETE	7.39	81.73
13,14-dihydro-15keto-PGD2	ND	41.15
13,14-dihydro-15keto-PGE2	10.07	41.15
13,14-dihydro-15-PGF2α	5.52	87.57
13HODE	5.60	61.22
14S-HDHA (14S-HDoHE)	10.33	85.01
15-deoxy-Δ12,14-PGJ2	ND	25.39
15epi-LXA4	ND	71.61
15HETE	7.38	85.01
15ketoPGE2	ND	80.09
17S-HDHA (17S-HDoHE)	11.98	85.01
20-OH-LTB4	ND	97.63
5HETE	7.71	73.15
5-oxoETE	16.40	68.73
6ketoPGF1alpha	9.00	97.63
6trans12epi LTB4	12.02	77.51
9HODE	11.02	61.22
LTB4	12.79	77.51
LTC4	ND	79.79
LTE4	ND	79.79
LXA4	ND	71.61
LXB4	ND	78.08
MaR1-	ND	80.46
PDx (10S,17S-DiHDHA)	ND	80.46
PGD2	12.59	42.81
PGE2	8.90	80.09
PGE3	ND	80.09
PGF2alpha	11.29	80.09
PGJ2	ND	41.15
RvD1	16.89	63.04
RvD2	ND	70.42
RvD3	ND	78.08
RvD4	ND	63.04
RvD5	ND	77.51
RvE1	ND	97.63
TXB2	11.18	36.14
TXB3	ND	36.14
Δ12-PGJ2	ND	41.15

Supplemental Table 5

	Tissue			Plasma	
Internal Standard	**CV (%)**	**Ext. efficiency (%)**		**CV (%)**	**Ext. efficiency**
RvE1-d4	3.04	74.88		7.91	113.08
TXB2-d4	1.15	35.42		5.91	75.90
PGE2-d4	13.84	64.18		6.21	93.67
RvD3-d5	16.31	64.07		8.56	106.99
PGD2-d4	13.81	46.98		8.44	72.86
RvD2-d5	24.95	49.68		7.01	103.78
LTC4-d5	14.09	11.91		14.12	92.02
13,14-dihydro-15-keto PGF2α-d4	8.08	61.30		7.98	99.70
LXA4-d5	22.32	48.68		7.05	89.13
RvD1-d5	22.59	51.06		7.80	103.59
13,14-dihydro-15-keto PGE2-d4	9.88	51.91		5.93	70.37
MaR1-d5	12.39	56.98		10.21	98.06
LTB4-d4	16.73	54.22		6.44	97.96
15d-PGJ2-d4	17.02	22.31		9.14	10.07
13HODE-d4	4.22	34.16		0.78	87.14
15HETEd8	14.80	48.88		6.05	98.04
12HETE-d8	14.42	43.02		5.88	93.38
5HETE-d8	14.97	56.13		7.30	99.47
5-oxo-ETE-d7	0.47	36.95		2.96	48.04

Supplemental Table 6

COX2 MKO/CCHF										
Intestine		MKO + CHOW		FLOX + CCHF		MKO + CCHF		MKO + CCHF + 4F		
Analyte	Analyte Group	AVG	SEM	AVG	SEM	AVG	SEM	AVG	SEM	P value ANOVA
PGE2	Pro-INF Pro-RES COX	**130.1049**	17.67697	**154.8545**	22.19736	**219.6015**	7.250831	**224.1641**	27.34117	**0.01100**
13,14-dihydro-15keto-PGE2	Pro-INF Pro-RES COX	**18.65562**	6.977379	**26.59384**	5.778491	**39.7527**	8.47639	**29.3641**	3.954735	0.18000
15ketoPGE2	Pro-INF Pro-RES COX	**4.821603**	0.340145	**3.007509**	0.418414	**5.729046**	0.811299	**6.43505**	1.434351	0.09000
13,14-dihydro-15keto-PGD2	Pro-INF Pro-RES COX	**0**	0	**0.436545**	0.085957	**0.625708**	0.109761	**0.34921**	0.041871	**0.00012**
PGD2	Pro-INF Pro-RES COX	**22.72576**	4.475025	**67.82052**	16.6129	**109.3332**	14.87925	**104.9495**	8.668743	**0.00038**
PGF2alpha	Pro-INF COX	**13.94984**	2.42389	**23.47068**	5.246906	**30.35665**	2.272336	**32.02882**	1.98113	**0.00446**
13,14-dihydro-15-PGF2alpha	Pro-INF COX	**3.045218**	1.306478	**3.581898**	0.381171	**4.802884**	0.849374	**4.440931**	0.759103	0.48000
6ketoPGF1alpha	Pro-INF COX	**885.3489**	166.1096	**874.6809**	126.9348	**1355.149**	75.31828	**1160.889**	87.63056	**0.02010**
TXB2	Pro-INF COX	**28.27415**	7.86846	**41.63473**	8.742927	**70.41658**	9.432695	**59.84675**	5.345416	**0.00731**
11HETE	Pro-INF COX	**302.9536**	64.97584	**208.4596**	23.30048	**292.5164**	18.46143	**269.0509**	14.70903	0.19200
TXB3	Pro-INF COX	**0.53394**	0.082182	**0.203565**	0.04731	**0.316546**	0.052343	**0.267723**	0.029074	**0.00398**
PGE3	Pro-INF COX	**2.416828**	0.516197	**0.896388**	0.147955	**1.552855**	0.161755	**1.028989**	0.092315	**0.00172**
LTE4	Pro-INF LOX	**3.199406**	1.78469	**3.98497**	1.434652	**2.34E+00**	0.314239	**2.116112**	0.630384	0.28300
LTC4	Pro-INF LOX	**0.145555**	0.065459	**0.021771**	0.017776	**0.12201**	0.056098	**0**	0	**0.04300**
LTB4	Pro-INF LOX	**0.184894**	0.051814	**0.523513**	0.22655	**0.502684**	0.129935	**1.340664**	0.475867	0.04100
6trans12epiLTB4	Pro-INF LOX	**1.436332**	0.161214	**5.581757**	1.487716	**8.002939**	1.363133	**7.396183**	1.876484	**0.02210**
20-OH-LTB4	Pro-INF LOX	NA		NA		NA		NA		
15HETE	Pro-INF LOX	**40.80628**	3.820122	**52.94731**	7.689674	**85.13183**	6.96146	**75.90653**	4.551297	**0.00020**
12HETE	Pro-INF LOX	**107.9613**	11.75757	**240.1011**	43.84243	**401.2302**	49.5114	**283.9585**	13.23646	**0.00015**
5HETE	Pro-INF LOX	**13.39223**	3.066657	**21.30335**	5.321729	**19.29686**	2.624429	**23.79374**	3.932442	0.21100
5oxoETE	Pro-INF LOX	**10.60884**	2.084198	**15.04229**	3.947132	**9.808143**	1.785673	**9.765037**	1.203819	0.37600
13HODE	Pro-INF LOX	**681.2591**	63.67992	**511.5074**	71.27692	**777.1342**	73.61072	**562.6813**	45.67362	**0.01100**
9HODE	Pro-INF LOX	**212.2021**	27.1653	**154.3053**	19.34346	**213.9067**	27.03916	**165.748**	21.88404	0.11000
PGJ2	Anit-INF COX	**0.305248**	0.046377	**2.023665**	0.457798	**2.55445**	0.320607	**1.487715**	0.22457	**0.00070**
delta12-PGJ2	Anit-INF COX	**0.347886**	0.037627	**1.588881**	0.332611	**2.016676**	0.245348	**1.268236**	0.181919	**0.00092**
15d-PGJ2	Anit-INF COX	**0.201174**	0.030139	**0.642379**	0.161375	**0.908851**	0.123036	**0.981466**	0.079195	**0.00053**
LXA4	Pro-RES LOX	**0.139316**	0.029291	**0.298082**	0.020151	**0.160693**	0.010314	**0.209938**	0.033679	**0.00290**
LXB4	Pro-RES LOX	**0.724377**	0.034944	**0.990643**	0.147032	**1.167727**	0.10755	**1.050134**	0.126834	**0.00775**
14HDHA	Pro-RES LOX	**56.15627**	2.041455	**55.13902**	8.292369	**60.14251**	4.646397	**73.99933**	7.394777	0.39000
MaR1	Pro-RES LOX	**0.833891**	0.037278	**1.945488**	0.525743	**2.001944**	0.245874	**2.111511**	0.431342	.048
17HDHA	Pro-RES LOX	**27.67051**	1.350567	**30.6692**	5.179139	**31.55328**	1.838325	**37.60557**	2.938465	0.21000
PDx	Pro-RES LOX	**1.814821**	0.043252	**3.349431**	0.732985	**3.913047**	0.28939	**4.320014**	0.709368	**0.00300**
RVD1	Pro-RES LOX	**0.019493**	0.003512	**0.014662**	0.002873	**0.007614**	0.003064	**0.01266**	0.001738	0.05100
RVD2	Pro-RES LOX	NA		NA		NA		NA		
RVD3	Pro-RES LOX	NA		NA		NA		NA		
RVD4	Pro-RES LOX	NA		NA		NA		NA		
RVD5	Pro-RES LOX	**0.224699**	0.009218	**0.346328**	0.076109	**0.45826**	0.110018	**0.620521**	0.089543	**0.01700**
RVE1	Pro-RES LOX	NA		NA		NA		NA		

Bolded ANOVA p-value = deemed a discovery/significant after FDR correction (see Supplemental Tables 8)

"NA" = not detected

(ng analyte/50 mg tissue)

Supplemental Table 7

COX2 MKO/CCHF										
Plasma		MKO + CHOW		FLOX + CCHF		MKO + CCHF		MKO + CCHF + 4F		
Analyte	Analyte Class	AVG	SEM	AVG	SEM	AVG	SEM	AVG	SEM	value ANOV
PGE2	Pro-INF Pro-RES COX	**0.1002126**	0.01254	**0.043826**	0.00697	**0.257758**	0.07335	**0.062081695**	0.010315	**0.00389**
13,14-dihydro-15keto-PGE2	Pro-INF Pro-RES COX	**0.0624112**	0.00844	**0.03482332**	0.01118	**0.091591**	0.03586	**0.035110351**	0.009715	0.187
15ketoPGE2	Pro-INF Pro-RES COX									
13,14-dihydro-15keto-PGD2	Pro-INF Pro-RES COX									
PGD2	Pro-INF Pro-RES COX	**0.0430357**	0.00463	**0.03142658**	0.00453	**0.121129**	0.03698	**0.049453065**	0.009514	**0.023**
PGF2alpha	Pro-INF COX	**0.0398516**	0.01226	**0.002**	0.00183	**0.172527**	0.03863	**0**	0	**5.27E-05**
13,14-dihydro-15-PGF2alpha	Pro-INF COX	**0.0173586**	0.00777	**0.03743635**	0.00389	**0.127788**	0.01794	**0.02671778**	0.010385	**1.46E-05**
6ketoPGF1alpha	Pro-INF COX	**0.1309958**	0.01804	**0.07581342**	0.00515	**1.779043**	0.79265	**0.255564707**	0.07099	**0.0258**
TXB2	Pro-INF COX	**2.5601606**	0.33835	**0.90714715**	0.2297	**6.964174**	1.6239	**0.296674794**	0.163183	**9.68E-05**
11HETE	Pro-INF COX	**1.2335002**	0.10851	**0.94764343**	0.08628	**4.546023**	1.30019	**0.890408289**	0.188157	**0.0027**
TXB3	Pro-INF COX	NA		NA		NA		NA		
PGE3	Pro-INF COX	NA		NA		NA		NA		
LTE4	Pro-INF LOX	NA		NA		NA		NA		
LTC4	Pro-INF LOX	NA		NA		NA		NA		
LTB4	Pro-INF LOX	NA		NA		NA		NA		
6trans12epiLTB4	Pro-INF LOX	**0.0091491**	0.00142	**0.01512863**	0.00492	**0.051592**	0.01777	**0.003125227**	0.002236	**0.00728**
20-OH-LTB4	Pro-INF LOX	NA		NA		NA		NA		
15HETE	Pro-INF LOX	**0.2563389**	0.02208	**0.29524656**	0.05387	**1.116653**	0.32715	**0.274306218**	0.051556	**0.00528**
12HETE	Pro-INF LOX	**6.6457207**	0.6605	**19.937009**	1.49592	**67.78914**	16.9543	**16.13547798**	4.176016	**0.000725**
5HETE	Pro-INF LOX	**0.3569618**	0.04818	**0.55062999**	0.05308	**1.006557**	0.12341	**0.669428065**	0.080441	**0.000523**
5oxoETE	Pro-INF LOX	**0.0619357**	0.00703	**0.14626461**	0.02571	**0.208111**	0.05709	**0.13861469**	0.061588	0.3458
13HODE	Pro-INF LOX	**16.409675**	1.76797	**24.0337481**	3.09993	**69.32201**	20.9973	**20.76155515**	3.011255	0.30458
9HODE	Pro-INF LOX	**3.5608511**	0.47297	**6.66813485**	1.08942	**11.73574**	2.37695	**4.624849755**	0.771352	**0.00339**
PGJ2	Anit-INF COX	NA		NA		NA		NA		
delta12-PGJ2	Anit-INF COX	NA		NA		NA		NA		
15d-PGJ2	Anit-INF COX	NA		NA		NA		NA		
LXA4	Pro-RES LOX	NA		NA		NA		NA		
LXB4	Pro-RES LOX	NA		NA		NA		NA		
14HDHA	Pro-RES LOX	**3.6227155**	0.41026	**2.67501931**	1.01009	**4.269966**	1.696	**3.720119211**	0.589758	0.791
MaR1	Pro-RES LOX									
17HDHA	Pro-RES LOX	**0.2147033**	0.03365	**0.28054228**	0.05388	**0.753965**	0.31687	**0.218589828**	0.050176	0.102
PDx	Pro-RES LOX	NA		NA		NA		NA		
RVD1	Pro-RES LOX	NA		NA		NA		NA		
RVD2	Pro-RES LOX	NA		NA		NA		NA		
RVD3	Pro-RES LOX	NA		NA		NA		NA		
RVD4	Pro-RES LOX	NA		NA		NA		NA		
RVD5	Pro-RES LOX	NA		NA		NA		NA		
RVE1	Pro-RES LOX	NA		NA		NA		NA		

Bolded ANOVA p-value = deemed significant/discovery after FDR correction (see Supplemental Table 9)
"NA" = not detected
(ng/100 µl plasma)

Supplemental Table 8

Order (i)	Analyte	P value one way ANOVA	i/m*α [α = 0.05]	P ≤ i/m*α
1	**13,14-dihydro-15keto-PGD2**	**0.000115**	**0.0015**	**Y**
2	**12HETE**	**0.000147**	**0.0030**	**Y**
3	**15HETE**	**0.000204**	**0.0045**	**Y**
4	**PGD2**	**0.000375**	**0.0061**	**Y**
5	**15d-PGJ2**	**0.000525**	**0.0076**	**Y**
6	**PGJ2**	**0.000700**	**0.0091**	**Y**
7	**delta12-PGJ2**	**0.000919**	**0.0106**	**Y**
8	**PGE3**	**0.001720**	**0.0121**	**Y**
9	**LXA4**	**0.002900**	**0.0136**	**Y**
10	**PDx**	**0.003000**	**0.0152**	**Y**
11	**TXB3**	**0.003980**	**0.0167**	**Y**
12	**PGF2alpha**	**0.004460**	**0.0182**	**Y**
13	**TXB2**	**0.007310**	**0.0197**	**Y**
14	**LXB4**	**0.007750**	**0.0212**	**Y**
15	**PGE2**	**0.011000**	**0.0227**	**Y**
16	**13HODE**	**0.011000**	**0.0242**	**Y**
17	**RVD5**	**0.017000**	**0.0258**	**Y**
18	**6ketoPGF1alpha**	**0.020100**	**0.0273**	**Y**
19	**6trans12epiLTB4**	**0.022100**	**0.0288**	**Y**
20	LTB4	0.041000	0.0303	N
21	LTC4	0.043000	0.0318	N
22	MaR1	0.048	0.0333	N
23	RVD1	0.051000	0.0348	N
24	15ketoPGE2	0.090000	0.0364	N
25	9HODE	0.110000	0.0379	N
26	13,14-dihydro-15keto-PGE2	0.180000	0.0394	N
27	11HETE	0.192000	0.0409	N
28	17HDHA	0.210000	0.0424	N
29	5HETE	0.211000	0.0439	N
30	LTE4	0.283000	0.0455	N
31	5oxoETE	0.376000	0.0470	N
32	14HDHA	0.390000	0.0485	N
33	13,14-dihydro-15-PGF2alpha	0.480000	0.0500	N

For each analyte, a P value was calculated by one-way ANOVA for *Cox2* MKO + CHOW, FLOX + CCHF, MKO + CCHF, and MKO + CCHF + 4F. Benjami-Hochberg procedure was applied to control FDR, with α = 0.05.

Supplemental Table 9

Order (i)	Analyte	P value one way ANOVA	i/m*α [α = 0.05]	P ≤ i/m*α
1	**13,14-dihydro-15keto-PGF2alpha**	**0.00001460**	**0.0029**	**Y**
2	**PGF2alpha**	**0.00005270**	**0.0059**	**Y**
3	**TXB2**	**0.00009680**	**0.0088**	**Y**
4	**5HETE**	**0.00052300**	**0.0118**	**Y**
5	**12HETE**	**0.00072500**	**0.0147**	**Y**
6	**11HETE**	**0.00270000**	**0.0176**	**Y**
7	**9HODE**	**0.00339000**	**0.0206**	**Y**
8	**PGE2**	**0.00389000**	**0.0235**	**Y**
9	**15HETE**	**0.00528000**	**0.0265**	**Y**
10	**6trans12epiLTB4**	**0.00728000**	**0.0294**	**Y**
11	**PGD2**	**0.02300000**	**0.0324**	**Y**
12	**6ketoPGF1alpha**	**0.02580000**	**0.0353**	**Y**
13	17HDHA	0.10180000	0.0382	N
14	13,14-dihydro-15keto-PGE2	0.18700000	0.0412	N
15	13HODE	0.30458000	0.0441	N
16	5oxoETE	0.34580000	0.0471	N
17	14HDHA	0.79110000	0.0500	N

For each analyte, a P value was calculated by one-way ANOVA for *Cox2* MKO + CHOW, FLOX + CCHF, MKO + CCHF, and MKO + CCHF + 4F. Benjami-Hochberg procedure was applied to control FDR at level α = 0.05.

Supplemental Table 10

Order (i)	Analyte	P value one way ANOVA	i/m*α [α = 0.05]	P ≤ i/m*α
1	**5oxoETE**	**0.000528**	**0.0015625**	**Y**
2	**TXB2**	**0.0042**	**0.003125**	**Y**
3	**LTB4**	**0.00493**	**0.0046875**	**Y**
4	**LTE4**	**0.005**	**0.00625**	**Y**
5	**13HODE**	**0.00518**	**0.0078125**	**Y**
6	**12HETE**	**0.00593**	**0.009375**	**Y**
7	15HETE	0.027	0.0109375	N
8	5HETE	0.0308	0.0125	N
9	6trans12epiLTB4	0.031	0.0140625	N
10	LXA4	0.035	0.015625	N
11	11HETE	0.038	0.0171875	N
12	TXB3	0.038	0.01875	N
13	PGE2	0.049	0.0203125	N
14	15d-PGJ2	0.12	0.021875	N
15	PGE3	0.13	0.0234375	N
16	15ketoPGE2	0.14	0.025	N
17	LXB4	0.143	0.0265625	N
18	LTC4	0.167	0.028125	N
19	PGD2	0.18	0.0296875	N
20	MaR1	0.243	0.03125	N
21	PDx	0.280	0.0328125	N
22	17HDHA	0.281	0.034375	N
23	RVD5	0.309	0.0359375	N
24	PGF2alpha	0.42	0.0375	N
25	13,14-dihydro-15keto-PGE2	0.5	0.0390625	N
26	PGJ2	0.53	0.040625	N
27	6ketoPGF1alpha	0.55	0.0421875	N
28	9HODE	0.615	0.04375	N
29	RVD1	0.630	0.0453125	N
30	13,14-dihydro-15keto-PGD2	0.72	0.046875	N
31	13,14-dihydro-15-PGF2alpha	0.95	0.0484375	N
32	14HDHA	0.973	0.05	N

For each analyte, a p value was calculated by one way ANOVA for *Il10*$^{-/-}$, PAC *Il10*$^{-/-}$, and PAC *Il10*$^{-/-}$ + 4F. Benjamini-Hochberg procedure was applied to control FDR at level α = 0.05.

Supplemental Table 11

PAC IL10								
Intestine		IL10		PAC IL10		PAC IL10 + 4F		
Analyte	Analyte Group	AVG	SEM	AVG	SEM	AVG	SEM	p-value ANOVA
PGE2	Pro-INF Pro-RES COX	**123.5036**	12.93743	**183.1655**	14.98647	**188.297**	17.65218	0.049
hydro-15ke	Pro-INF Pro-RES COX	**5.316031**	0.710741	**6.175738**	0.880435	**7.479119**	1.525962	0.5
L5ketoPGE2	Pro-INF Pro-RES COX	**3.112133**	0.920724	**2.220529**	0.17067	**5.078026**	1.469098	0.14
hydro-15ke	Pro-INF Pro-RES COX	**0.113975**	0.007944	**0.123809**	0.012269	**0.13599**	0.023366	0.72
PGD2	Pro-INF Pro-RES COX	**82.6436**	8.321074	**115.5792**	10.26302	**105.6904**	11.70313	0.18
PGF2alpha	Pro-INF COX	**35.30197**	4.335548	**42.52921**	3.420139	**34.85619**	5.482543	0.42
13,14-dihydro-15-PGF2alpha	Pro-INF COX	**1.404186**	0.265176	**1.274416**	0.258082	**1.288082**	0.326297	0.95
6ketoPGF1alpha	Pro-INF COX	**824.1543**	60.77948	**961.1142**	74.83163	**980.1358**	114.866	0.55
TXB2	Pro-INF COX	**22.79672**	2.557763	**50.77635**	4.912987	**53.33701**	6.363669	**0.0042**
11HETE	Pro-INF COX	**141.2866**	9.433039	**188.0841**	9.982078	**180.6064**	13.41702	0.038
TXB3	Pro-INF COX	**0.14739**	0.019933	**0.554818**	0.096909	**0.474485**	0.099649	0.038
PGE3	Pro-INF COX	**3.839775**	0.69742	**6.167248**	0.795111	**6.292541**	0.780001	0.13
LTE4	Pro-INF LOX	**0.822888**	0.249781	**2.658975**	0.395416	**1.325573**	0.350312	**0.005**
LTC4	Pro-INF LOX	**0.307262**	0.080549	**0.397281**	0.054057	**0.258885**	0.035752	0.167
LTB4	Pro-INF LOX	**0.049968**	0.00865	**0.57657**	0.155281	**0.16748**	0.060947	**0.00493**
ans12epiLT	Pro-INF LOX	**0.14739**	0.019933	**0.554818**	0.096909	**0.449521**	0.094329	0.031
20-OH-LTB4	Pro-INF LOX	ND		NA		NA		
15HETE	Pro-INF LOX	**23.60197**	2.749026	**36.1296**	1.900285	**34.56993**	3.329698	0.027
12HETE	Pro-INF LOX	**52.03024**	5.644736	**100.1864**	10.81897	**70.2806**	4.532052	**0.00593**
5HETE	Pro-INF LOX	**3.540868**	0.578416	**7.343705**	0.963924	**5.605692**	0.694329	0.0308
5oxoETE	Pro-INF LOX	**2.475791**	0.479318	**5.79136**	0.916129	**2.377679**	0.215895	**0.000528**
13HODE	Pro-INF LOX	**451.1757**	51.55797	**649.9629**	60.02646	**435.9803**	39.97587	**0.00518**
9HODE	Pro-INF LOX	**200.3926**	29.0203	**257.6375**	35.31335	**267.5777**	54.10945	0.615
PGJ2	Anit-INF COX	**1.074836**	0.10452	**1.333422**	0.16271	**1.35348**	0.176848	0.53
lelta12-PGJ	Anit-INF COX							
15d-PGJ2	Anit-INF COX	**0.987922**	0.145539	**1.538454**	0.181092	**1.586446**	0.237887	0.12
LXA4	Pro-RES LOX	**0.099407**	0.014436	**0.231527**	0.033318	**0.137448**	0.012186	0.035
LXB4	Pro-RES LOX	**3.540868**	0.578416	**5.296276**	0.563212	**5.605692**	0.694329	0.143
14HDHA	Pro-RES LOX	**26.50432**	13.2845	**24.46778**	3.488511	**25.89934**	4.575421	0.973
MaR1	Pro-RES LOX	**0.279022**	0.037226	**0.504185**	0.09352	**0.507511**	0.096215	.243
17HDHA	Pro-RES LOX	**12.40136**	1.736456	**19.04**	3.119583	**17.56134**	2.089999	0.281
PDx	Pro-RES LOX	**0.757618**	0.11111	**1.235678**	0.205752	**1.303258**	0.247282	0.280
RVD1	Pro-RES LOX	**0.011276**	0.001656	**0.008822**	0.001744	**0.009979**	0.001427	0.630
RVD2	Pro-RES LOX	**NA**		**NA**		**NA**		
RVD3	Pro-RES LOX	**NA**		**NA**		**NA**		
RVD4	Pro-RES LOX	**NA**		**NA**		**NA**		
RVD5	Pro-RES LOX	**0.0669**	0.009743	**0.11999**	0.031211	**0.144472**	0.034097	0.309
RVE1	Pro-RES LOX	**NA**		**NA**		**NA**		

Bolded ANOVA p-value = significant/discovery after FDR correction (see Supplemental Table 10).
"NA" = not detected
(ng/50 mg tissue)

Supplemental Table 12

Pro-INF LOX							***Pro-INF COX***					
	IL10+PX		IL10+PX+4F					IL10+PX		IL10+PX+4F		
	AVG	SEM	**AVG**	SEM	*TTEST*			**AVG**	SEM	**AVG**	SEM	*TTEST*
20-OH-LTB4	**ND**		**ND**				**6ketoPGF1α**	**0.08**	0.06	**0.02**	0.00	0.319
LTC4	**0.03**	0.00	**0.00**	0.00	3.05E-06		**TXB3**	**ND**		**ND**		
LTE4	**0.02**	0.00	**0.00**	0.00	2.42E-05		**TXB2**	**1.41**	0.52	**0.67**	0.27	0.270
6trans12epi LTB4	**2.71**	1.90	**0.07**	0.01	0.159		**PGE3**	**ND**		**ND**		
LTB4	**ND**		**ND**				**PGF2α**	**0.17**	0.04	**0.05**	0.01	0.043
13HODE	**86.81**	32.72	**15.37**	1.51	0.037		**13,14-dihydro-15-PGF2α**	**0.03**	0.00	**0.01**	0.00	0.041
9HODE	**82.48**	35.90	**12.76**	1.72	0.054		**11HETE**	**7.63**	4.09	**0.88**	0.16	0.164
15HETE	**10.13**	4.96	**1.22**	0.17	0.116		**Total**	**9.28**	3.95	**1.63**	0.33	0.109
12HETE	**34.95**	8.19	**8.72**	2.12	0.004							
5HETE	**33.05**	15.77	**5.82**	1.12	0.110		***Pro-RES LOX***					
5-oxoETE	**1.06**	0.62	**0.11**	0.02	*0.059*			IL10+PX		IL10+PX+4F		
Total	**154.83**	49.41	**43.93**	4.93	0.033			**AVG**	SEM	**AVG**	SEM	*TTEST*
							RvE1	**ND**		**ND**		
PGE2/PGD2							**RvD3**	**ND**		**ND**		
	IL10+PX		IL10+PX+4F				**LXB4**	**ND**		**ND**		
	AVG	SEM	**AVG**	SEM	*TTEST*		**RvD2**	**ND**		**ND**		
PGE2	**0.36**	0.17	**0.07**	0.01	0.144		**LXA4**	**0.36**	0.18	**0.07**	0.01	0.176
PGD2	**0.34**	0.16	**0.07**	0.01	0.143		**15epi-LXA4**	**0.26**	0.12	**0.05**	0.01	0.140
15ketoPGE2	**0.04**	0.01	**0.02**	0.00	0.029		**RvD1**	**0.13**	0.06	**0.02**	0.00	0.110
13,14-dihydro-15keto-PGE2	**ND**		**ND**				**RvD4**	**ND**		**ND**		
13,14-dihydro-15keto-PGD2	**0.13**	0.05	**0.02**	0.00	*0.095*		**MaR1-**	**2.67**	1.52	**0.05**	0.02	0.147
Total	**0.84**	0.38	**0.42**	0.13	0.134		**PDx**	**3.22**	1.85	**0.07**	0.02	0.151
							RvD5	**2.11**	1.11	**0.10**	0.02	0.131
Anti-INF COX							**17HDHA**	**14.49**	1.95	**6.52**	1.46	0.027
	IL10+PX		IL10+PX+4F				**14HDHA**	**11.17**	2.23	**4.42**	0.72	0.036
	AVG	SEM	**AVG**	SEM	*TTEST*		**Total**	**26.44**	4.22	**10.97**	4.48	0.03
PGJ2	**0.03**	0.00	**0.02**	0.00	0.166							
Δ12-PGJ2	**0.98**	0.45	**0.18**	0.03	0.138							
15-deoxy-Δ12,14-PGJ2	**ND**		**ND**									
Total	**9.914**	4.579	**1.833**	0.293	0.139							

(ng/100 µl plasma)

1. Masoodi M, Mir AA, Petasis NA, Serhan CN, and Nicolaou A. Simultaneous lipidomic analysis of three families of bioactive lipid mediators leukotrienes, resolvins, protectins and related hydroxy-fatty acids by liquid chromatography/electrospray ionisation tandem mass spectrometry. *Rapid Commun Mass Spectrom.* 2008;22(2):75-83.
2. Dalli J, and Serhan CN. Specific lipid mediator signatures of human phagocytes: microparticles stimulate macrophage efferocytosis and pro-resolving mediators. *Blood.* 2012;120(15):e60-72.
3. Colas RA, Shinohara M, Dalli J, Chiang N, and Serhan CN. Identification and signature profiles for pro-resolving and inflammatory lipid mediators in human tissue. *Am J Physiol Cell Physiol.* 2014;307(1):C39-54.
4. Le Faouder P, Baillif V, Spreadbury I, Motta JP, Rousset P, Chene G, et al. LC-MS/MS method for rapid and concomitant quantification of pro-inflammatory and pro-resolving polyunsaturated fatty acid metabolites. *J Chromatogr B Analyt Technol Biomed Life Sci.* 2013;932:123-33.
5. Viola JR, Lemnitzer P, Jansen Y, Csaba G, Winter C, Neideck C, et al. Resolving Lipid Mediators Maresin 1 and Resolvin D2 Prevent Atheroprogression in Mice. *Circ Res.* 2016;119(9):1030-8.
6. Homann J, Suo J, Schmidt M, de Bruin N, Scholich K, Geisslinger G, et al. In Vivo Availability of Pro-Resolving Lipid Mediators in Oxazolone Induced Dermal Inflammation in the Mouse. *PLoS One.* 2015;10(11):e0143141.
7. Buczynski MW, Dumlao DS, and Dennis EA. Thematic Review Series: Proteomics. An integrated omics analysis of eicosanoid biology. *J Lipid Res.* 2009;50(6):1015-38.
8. Lawrence T, Willoughby DA, and Gilroy DW. Anti-inflammatory lipid mediators and insights into the resolution of inflammation. *Nat Rev Immunol.* 2002;2(10):787-95.
9. Buckley CD, Gilroy DW, and Serhan CN. Proresolving lipid mediators and mechanisms in the resolution of acute inflammation. *Immunity.* 2014;40(3):315-27.
10. Serhan CN. Pro-resolving lipid mediators are leads for resolution physiology. *Nature.* 2014;510(7503):92-101.
11. Mozurkewich EL, Greenwood M, Clinton C, Berman D, Romero V, Djuric Z, et al. Pathway Markers for Pro-resolving Lipid Mediators in Maternal and Umbilical Cord Blood: A Secondary Analysis of the Mothers, Omega-3, and Mental Health Study. *Front Pharmacol.* 2016;7:274.
12. Norris PC, Gosselin D, Reichart D, Glass CK, and Dennis EA. Phospholipase A2 regulates eicosanoid class switching during inflammasome activation. *Proc Natl Acad Sci U S A.* 2014;111(35):12746-51.
13. Health UDo, and Services H. Guidance for industry, bioanalytical method validation. *http://wwwfdagov/cder/guidance/indexhtm.* 2001.
14. N.W. Daae L, and Bremer J. The acylation of glycerophosphate in rat liver A new assay procedure for glycerophosphate acylation, studies on its subcellular and submitochondrial localization and determination of the reaction products. *Biochimica et Biophysica Acta (BBA) - Lipids and Lipid Metabolism.* 1970;210(1):92-104.
15. Lahar N, Lei NY, Wang J, Jabaji Z, Tung SC, Joshi V, et al. Intestinal subepithelial myofibroblasts support in vitro and in vivo growth of human small intestinal epithelium. *PLoS One.* 2011;6(11):e26898.
16. Rouch JD, Scott A, Lei NY, Solorzano-Vargas RS, Wang J, Hanson EM, et al. Development of Functional Microfold (M) Cells from Intestinal Stem Cells in Primary Human Enteroids. *PLoS One.* 2016;11(1):e0148216.
17. Watanabe J, Lin JA, Narasimha AJ, Shahbazian A, Ishikawa TO, Martin MG, et al. Novel anti-inflammatory functions for endothelial and myeloid cyclooxygenase-2 in a new mouse model of Crohn's disease. *Am J Physiol Gastrointest Liver Physiol.* 2010;298(6):G842-50.

18. Holgersen K, Kvist PH, Markholst H, Hansen AK, and Holm TL. Characterisation of enterocolitis in the piroxicam-accelerated interleukin-10 knock out mouse--a model mimicking inflammatory bowel disease. *J Crohns Colitis.* 2014;8(2):147-60.
19. Kubica P, Kot-Wasik A, Wasik A, Namiesnik J, and Landowski P. Modern approach for determination of lactulose, mannitol and sucrose in human urine using HPLC-MS/MS for the studies of intestinal and upper digestive tract permeability. *J Chromatogr B Analyt Technol Biomed Life Sci.* 2012;907:34-40.
20. Meddings JB, and Gibbons I. Discrimination of site-specific alterations in gastrointestinal permeability in the rat. *Gastroenterology.* 1998;114(1):83-92.
21. Gupta J, and Nebreda AR. Analysis of Intestinal Permeability in Mice. *Bio-protocol.* 2014;4(22):e1289.
22. Volynets V, Reichold A, Bardos G, Rings A, Bleich A, and Bischoff SC. Assessment of the Intestinal Barrier with Five Different Permeability Tests in Healthy C57BL/6J and BALB/cJ Mice. *Dig Dis Sci.* 2016;61(3):737-46.
23. Jilling T, Lu J, Jackson M, and Caplan MS. Intestinal Epithelial Apoptosis Initiates Gross Bowel Necrosis in an Experimental Rat Model of Neonatal Necrotizing Enterocolitis. *Pediatr Res.* 2004;55(4):622-9.
24. Erben U, Loddenkemper C, Doerfel K, Spieckermann S, Haller D, Heimesaat MM, et al. A guide to histomorphological evaluation of intestinal inflammation in mouse models. *International journal of clinical and experimental pathology.* 2014;7(8):4557-76.
25. Williams KL, Fuller CR, Dieleman LA, DaCosta CM, Haldeman KM, Sartor RB, et al. Enhanced survival and mucosal repair after dextran sodium sulfate–induced colitis in transgenic mice that overexpress growth hormone. *Gastroenterology.* 2001;120(4):925-37.
26. Ivanov, II, Frutos Rde L, Manel N, Yoshinaga K, Rifkin DB, Sartor RB, et al. Specific microbiota direct the differentiation of IL-17-producing T-helper cells in the mucosa of the small intestine. *Cell Host Microbe.* 2008;4(4):337-49.
27. Olson MA, Lee MS, Kissner TL, Alam S, Waugh DS, and Saikh KU. Discovery of small molecule inhibitors of MyD88-dependent signaling pathways using a computational screen. *Sci Rep.* 2015;5:14246.
28. Huang WY, Gong X, Zhang L, Jiang R, Kuang G, Wang B, et al. *BML-111 ameliorates endotoxin-induced liver injury through increasing prostaglandin J2 production via ERK/COX2 pathway.* 2017.
29. Zhou XY, Yu ZJ, Yan D, Wang HM, Huang YH, Sha J, et al. BML-11, a lipoxin receptor agonist, protected carbon tetrachloride-induced hepatic fibrosis in rats. *Inflammation.* 2013;36(5):1101-6.
30. York AG, Williams KJ, Argus JP, Zhou QD, Brar G, Vergnes L, et al. Limiting Cholesterol Biosynthetic Flux Spontaneously Engages Type I IFN Signaling. *Cell.* 2015;163(7):1716-29.
31. Ng CJ, Bourquard N, Grijalva V, Hama S, Shih DM, Navab M, et al. Paraoxonase-2 Deficiency Aggravates Atherosclerosis in Mice Despite Lower Apolipoprotein-B-containing Lipoproteins: ANTI-ATHEROGENIC ROLE FOR PARAOXONASE-2. *Journal of Biological Chemistry.* 2006;281(40):29491-500.
32. Hu ZD, Wei TT, Tang QQ, Ma N, Wang LL, Qin BD, et al. Gene expression profile of THP-1 cells treated with heat-killed Candida albicans. *Ann Transl Med.* 2016;4(9):170.
33. Park EK, Jung HS, Yang HI, Yoo MC, Kim C, and Kim KS. Optimized THP-1 differentiation is required for the detection of responses to weak stimuli. *Inflammation research : official journal of the European Histamine Research Society [et al].* 2007;56(1):45-50.

34. Vladykovskaya E, Ozhegov E, Hoetker JD, Xie Z, Ahmed Y, Suttles J, et al. Reductive metabolism increases the proinflammatory activity of aldehyde phospholipids. *Journal of lipid research.* 2011;52(12):2209-25.
35. Lipinski S, Till A, Sina C, Arlt A, Grasberger H, Schreiber S, et al. DUOX2-derived reactive oxygen species are effectors of NOD2-mediated antibacterial responses. *Journal of Cell Science.* 2009;122(19):3522-30.
36. Wang Y, Sawashita J, Qian J, Zhang B, Fu X, Tian G, et al. ApoA-I deficiency in mice is associated with redistribution of apoA-II and aggravated AApoAII amyloidosis. *J Lipid Res.* 2011;52(8):1461-70.
37. Guirgis FW, Leeuwenburgh C, Grijalva V, Bowman J, Kalynych C, Moldawer L, et al. HDL Cholesterol Efflux is Impaired in Older Patients with Early Sepsis: A Subanalysis of a Prospective Pilot Study. *Shock (Augusta, Ga).* 2017.
38. Meriwether D, Imaizumi S, Grijalva V, Hough G, Vakili L, Anantharamaiah GM, et al. Enhancement by LDL of transfer of L-4F and oxidized lipids to HDL in C57BL/6J mice and human plasma. *J Lipid Res.* 2011;52(10):1795-809.
39. Metsalu T, and Vilo J. ClustVis: a web tool for visualizing clustering of multivariate data using Principal Component Analysis and heatmap. *Nucleic Acids Res.* 2015;43(W1):W566-70.

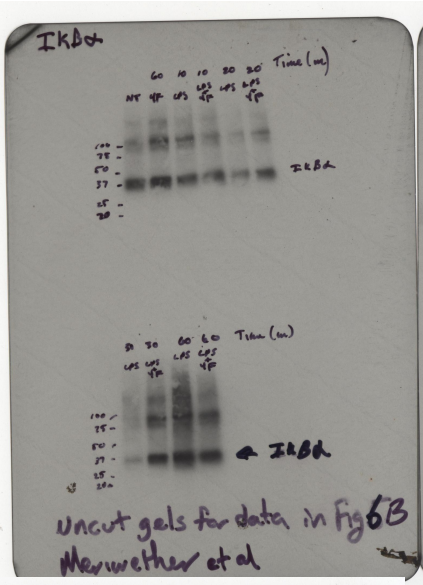

uncut gels for data in Fig 6B
Meriwether et al

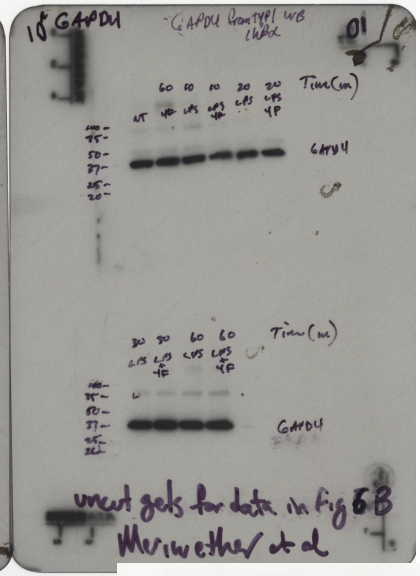

uncut gels for data in Fig 6B
Meriwether et al

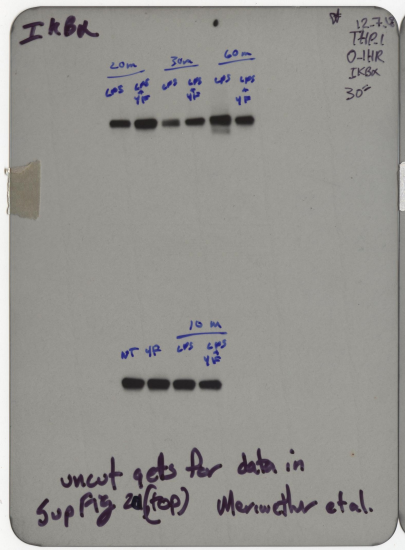

uncut gels for data in
Sup Fig 2a (top) Meriwether et al.

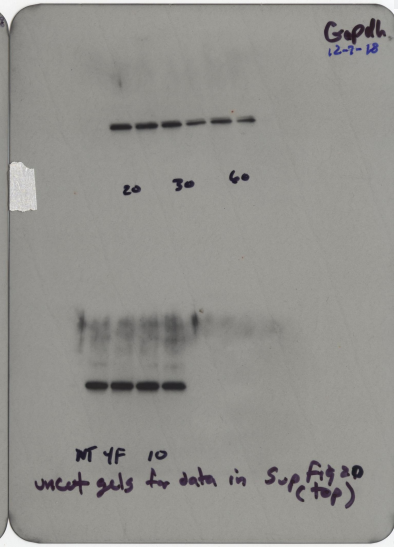

NT YF 10
uncut gels for data in Sup Fig 2D (top)

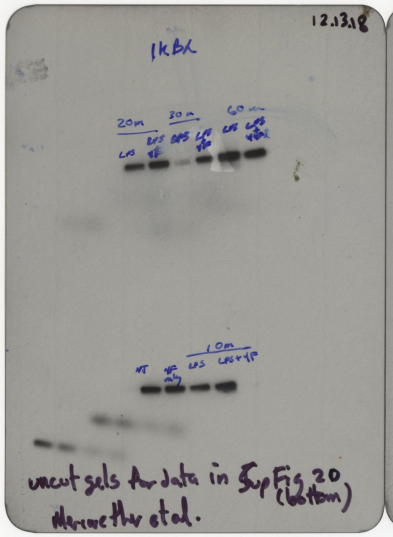

uncut gels for data in Sup Fig 2D (bottom)
Meriwether et al.

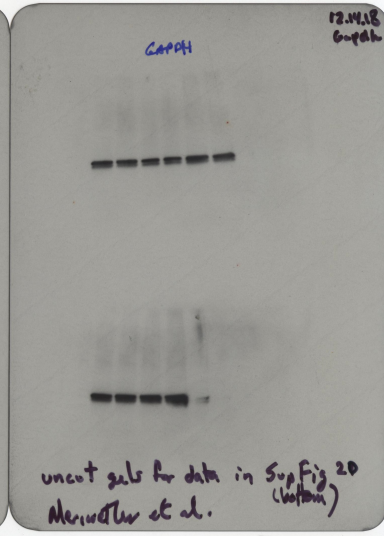

uncut gels for data in Sup Fig 2D (bottom)
Meriwether et al.